Published in final edited form as:

*Sci Transl Med*. 2020 May 06; 12(542): . doi:10.1126/scitranslmed.aax4517.

# BCG vaccination–induced emergency granulopoiesis provides rapid protection from neonatal sepsis

**Byron Brook**[1], **Danny J. Harbeson**[1], **Casey P. Shannon**[2,3], **Bing Cai**[4], **Daniel He**[1,2,3], **Rym Ben-Othman**[4], **Freddy Francis**[1], **Joe Huang**[4], **Natallia Varankovich**[4], **Aaron Liu**[1], **Winnie Bao**[4], **Morten Bjerregaard-Andersen**[5,6,7], **Frederik Schaltz-Buchholzer**[5,6,8], **Lilica Sanca**[5], **Christian N. Golding**[5,6], **Kristina Lindberg Larsen**[5,6], **Ofer Levy**[9,10,11], **Beate Kampmann**[12,13], **The EPIC Consortium***, **Rusung Tan**[14], **Adrian Charles**[14], **James L. Wynn**[15], **Frank Shann**[16], **Peter Aaby**[5], **Christine S. Benn**[5,6,8], **Scott J. Tebbutt**[2,3,17], **Tobias R. Kollmann**[1,4,18,†,‡], **Nelly Amenyogbe**[1,18,†,‡]

[1]Department of Experimental Medicine, University of British Columbia, 2775 Laurel Street, 10th Floor, Room 10117, Vancouver, BC V5Z 1M9, Canada.

[2]PROOF Centre of Excellence, British Columbia, 10th floor, 1190 Hornby Street, Vancouver, BC V6Z 2K5, Canada.

[3]UBC Centre for Heart Lung Innovation, St. Paul's Hospital, 1081 Burrard Street, Vancouver, BC V6Z 1Y6, Canada.

[4]Department of Pediatrics, University of British Columbia, and BC Children's Hospital, 4480 Oak Street, Vancouver, BC V6H 3V4, Canada.

[5]Bandim Health Project, Indepth Network, Apartado 861, 1004 Bissau, Guinea-Bissau.

[6]Research Center for Vitamins and Vaccines (CVIVA), Statens Serum Institut (SSI), Artillerivej 5, 2300 Copenhagen S, Denmark.

*The Expanded Program on Immunization (EPIC) Consortium collaborators and affiliations appear at the end of this paper.



‡Corresponding author. n.akuvy@gmail.com (N.A.); tkollm@mac.com (T.R.K.).
†These authors contributed equally to this work.

**Author contributions:** N.A. and T.R.K. developed the overall idea and study design. N.A., T.R.K., B.B., D.J.H., S.J.T., R.B.O., and J.L.W. contributed to the design of the mouse studies, with B.B., N.A., D.J.H., B.C., D.H., F.F., J.H., N.V., A.L., W.B., R.T., and A.C. executing the animal experiments that generated the mouse data. P.A., C.S.B., M.B.-A., F.S.-B., F.S., N.A., and T.R.K. designed the BCGIMED immune study, with L.S., C.N.G., and K.L.L. contributing to the sample processing and data generation. O.L., B.K., and T.R.K. designed the EPIC study, with the EPIC Consortium generating the human data from The Gambia and PNG presented in Fig. 4. B.B., N.A., C.P.S., S.J.T., D.J.H., D.H., and T.R.K. contributed to the overall data analysis. All authors contributed to the writing of the manuscript.

**Competing interests:** J.L.W. has consulted for Evolve Biosystems, assisting with the definition of neonatal sepsis. O.L. is a named inventor on several patents related to vaccine adjuvants (WO2019099564, Novel Imidazopyrimidine compounds and uses thereof) and has also been an expert consultant for Wilmington Trust. All other authors declare that they have no competing interests.

**Data and materials availability:** The EPIC data described here for Gambia and PNG pilot cohorts were deposited in the National Center for Biotechnology Information Gene Expression Omnibus Repository with the dataset identifiers GSE111404 and GSE123070, and in ImmPort (http://immport.niaid.nih.gov) under accession numbers SDY1256 and SDY1412. Access to the BCGIMED data from Guinea-Bissau can be requested by email from C.S.B (cb@ssi.dk). The mouse knockout strains for G-CSF and S100A9 were provided with material transfer agreements from laboratories indicated in Materials and Methods. All data associated with this study are present in the paper or the Supplementary Materials.

SUPPLEMENTARY MATERIALS
stm.sciencemag.org/cgi/content/full/12/542/eaax4517/DC1.

[7]Department of Endocrinology, Odense University Hospital, Kløvervænget 6, 5000 Odense C, Denmark.

[8]OPEN, Institute of Clinical Research and Danish Institute for Advanced Science, University of Southern Denmark, and Odense University Hospital, J.B. Winslóws Vej, 5000 Odense C, Denmark.

[9]Precision Vaccines Program, Boston Children's Hospital, Boston, MA 02115, USA.

[10]Harvard Medical School, Boston, MA 02115, USA.

[11]Broad Institute of MIT and Harvard, Cambridge, MA 02142, USA.

[12]Vaccines and Immunity Theme, Medical Research Council Unit, The Gambia at the London School of Hygiene and Tropical Medicine, Atlantic Boulevard, P.O. Box 273, Banjul, The Gambia.

[13]Vaccine Centre, Faculty of Infectious and Tropical Diseases, London School of Hygiene and Tropical Medicine, London WC1E 7HT, UK.

[14]Department of Pathology, Sidra Medicine and Weill Cornell Medicine, Doha, Qatar.

[15]Department of Paediatrics and Department of Pathology, Immunology, and Laboratory Medicine, University of Florida, P.O. Box 100296, Gainesville, FL 32610-0296, USA.

[16]Department of Paediatrics, University of Melbourne, Melbourne, VIC 3052, Australia.

[17]Department of Medicine, Division of Respiratory Medicine, University of British Columbia, Vancouver, BC V5Z 1M9, Canada.

[18]Telethon Kids Institute, 100 Roberts Road, Subiaco, Western Australia 6008, Australia.

## Abstract

Death from sepsis in the neonatal period remains a serious threat for millions. Within 3 days of administration, bacille Calmette-Guérin (BCG) vaccination can reduce mortality from neonatal sepsis in human newborns, but the underlying mechanism for this rapid protection is unknown. We found that BCG was also protective in a mouse model of neonatal polymicrobial sepsis, where it induced granulocyte colony-stimulating factor (G-CSF) within hours of administration. This was necessary and sufficient to drive emergency granulopoiesis (EG), resulting in a marked increase in neutrophils. This increase in neutrophils was directly and quantitatively responsible for protection from sepsis. Rapid induction of EG after BCG administration also occurred in three independent cohorts of human neonates.

## INTRODUCTION

Neonatal death remains a serious threat, currently comprising nearly half of all under 5-year-old mortality (1). Among the causes of neonatal death, infections are prominent, leading to an estimated 1.6 million neonatal deaths every year (2, 3). The most severe and overwhelming form of neonatal infection is sepsis, most commonly striking during the first few days of life (4-6). Although a microbial cause for neonatal sepsis is identified in only one-fifth of cases, the list of possibly causative pathogens is not only long but also varies between populations (7-9). This poses considerable difficulty in providing protection from

neonatal sepsis through pathogen-specific vaccination. A pathogen-agnostic approach to broadly protect from neonatal sepsis is urgently needed.

Neonatal bacille Calmette-Guérin (BCG) vaccination can reduce overall neonatal mortality in addition to tuberculosis, variably referred to as BCG's beneficial heterologous, off-target, nonspecific, or pathogen-agnostic effect (10, 11). In a meta-analysis of three randomized controlled trials comprising 6544 high-risk neonates in low-resource settings, BCG-Denmark administered shortly after birth reduced overall mortality in the first 28 days of life by 38% [95% confidence interval (CI), 17 to 54%] and the in-hospital sepsis case fatality by 54% (2 to 78%); of note, a 45% decrease in mortality was already detected in the first 3 days after BCG administration (6, 10). The mechanisms for BCG's pathogen-agnostic protective effects have not been established but have been hypothesized to possibly involve cross-reactive T cells and/or activation of innate immunity (12, 13). Given the substantial public health implications of neonatal infection and BCG's beneficial nonspecific effects, understanding the underlying mechanisms is extremely important (14-17).

## RESULTS

### BCG vaccination was protective against polymicrobial sepsis

To identify the mechanism of BCG's nonspecific effects, we tested BCG in a well-established murine neonatal sepsis model in which we subcutaneously administered 50 μl of BCG-Denmark (Statens Serum Institute) to neonatal mice [day of life (DOL) 4 to 5], followed 3 days later by intraperitoneally injected cecal slurry (CS) to induce polymicrobial sepsis (18-23). We found that BCG markedly improved survival in neonatal mice as it does in humans (Fig. 1A and data file S1). BCG-mediated protection was, however, time limited after neonatal vaccination, and it no longer conferred protection when challenge was delayed by 10 to 12 days (fig. S1A). BCG-induced protection was also dependent on the age of administration, such that mice vaccinated in the juvenile period (preweaning; DOL 17 to 18) were protected, whereas adult mice immunized at 6 weeks of life were not protected when challenged 3 days after BCG (fig. S1, B and C).

Neonatal BCG vaccination was associated with decreased production of potentially harmful inflammatory cytokines (Fig. 1B and fig. S2A) and reduced bacterial load in blood and organs 24 hours into sepsis (Fig. 1C). The beneficial effect of BCG could, thus, have resulted from directly reducing bacterial load, from preventing harmful inflammatory responses during sepsis, or both (24). Lipopolysaccharide (LPS)–induced neonatal death, which we have previously shown to be due to inflammation (19), was used to assess whether BCG's protective effect was related to inflammation. Specifically, we broadly measured plasma cytokine production in BCG-vaccinated and control mice 3 days after BCG (prechallenge) and 24 or 12 hours after intraperitoneal challenge with either CS or LPS to identify the changes immediately before mortality in the two challenge models (Fig. 1D). Principal components analysis (PCA) revealed substantial differences in cytokine production between pre- and postchallenge samples [PC1; 61.7% of variance explained between pre- and postchallenge (CS and LPS) and between challenge type in postchallenge samples (PC2; 9.5% of variance explained between CS and LPS)]. Nevertheless, although cytokine responses to challenge with CS differed between BCG and control pups, the cytokine profile

after LPS challenge was not affected by BCG. BCG also did not protect mice from intraperitoneally injected LPS-induced endotoxin shock and death (Fig. 1, E and F, and fig. S2B). This suggests that BCG's protective effect against CS challenge was not the primary result of an altered host inflammatory response but mediated by another mechanism such as antimicrobial effector function.

## BCG-induced increase in neutrophils was required and sufficient for protection from sepsis

Antimicrobial effector functions can be broadly divided into cellular and humoral mechanisms (25). We hypothesized that neutrophils, among the most rapidly acting innate antimicrobial effector cells (26), might play a central role in BCG-induced protection. Neutrophil populations in the spleen, a hematopoietic organ in the neonate, changed markedly after BCG vaccination, with increased immature neutrophils detectable 2 to 3 days after vaccination, followed by mature neutrophils on day 3 after vaccination; these were released from the spleen 24 hours after challenge (Fig. 2A; gating strategy in fig. S3). We found that the BCG-induced reduction in bacterial burden (24-hour post-CS challenge) was transferable to naïve recipients by adoptive transfer of the cellular compartment from BCG-vaccinated donor spleens 3 days after vaccination, the same time frame that conferred the survival benefit (Fig. 2B). This supported the hypothesis of important cellular antimicrobial mechanisms. To directly examine the role of mature neutrophils, we used both neutrophil depletion (positive selection of mature neutrophils via magnetic antibody labeling of $Ly6G^+$ cells) and purification (negative selection of mature neutrophils via magnetic antibody labeling of all other cells) to determine whether the BCG-induced increase in neutrophils was necessary and/or sufficient to provide the observed protection (adoptive transfer strategy in fig. S4). We found that adoptive transfer of neutrophil-depleted spleens did not protect (Fig. 2B and fig. S5A), yet transfer of purified mature neutrophils did (Fig. 2C and fig. S5B). Furthermore, scaling up the number of mature control neutrophils to match the number present in a BCG-vaccinated donor spleen or, conversely, scaling down the number of neutrophils in a BCG-vaccinated donor spleen to match the number present in the control donor spleens, provided the same degree of protection (Fig. 2C and fig. S5B). This indicated that the increase in mature neutrophils directly correlated with BCG's beneficial effect in reducing mortality upon sepsis challenge.

The ability of BCG to protect different age groups and the duration of protection reflected the age-dependent ability of BCG to induce mature neutrophil expansion. Vaccination in early life (DOL 4 to 5) followed by delay of challenge to DOL 16 to 17 showed no BCG-induced neutrophil expansion or protection (figs. S1A and S6A). However, both protection against CS-induced mortality and BCG-induced neutrophil expansion were observed in juvenile mice administered BCG on DOL 18 (figs. S1B and S6B). BCG did not protect adult mice from sepsis, nor was any neutrophil expansion observed after BCG administration to adult animals, further confirming the association of neutrophil expansion with BCG's ability to protect (figs. S1C and S6, C and D). This points to a narrow and specific window of opportunity around birth for BCG to exert its protection from polymicrobial sepsis.

Although neutrophil expansion after BCG vaccination was associated with bacterial clearance (Fig. 1C), it could also potentially induce harm (27, 28). Despite greater neutrophil recruitment into the lungs 24 hours after challenge of previously BCG-vaccinated mice, no notable pathological differences were observed between the lungs of control and BCG-vaccinated mice (fig. S7, A to I). Instead, the number of neutrophils recruited to the lung correlated with reduced bacterial burden, as well as accelerated weight recovery postchallenge (fig. S7J and K), both established markers of improved outcome in this model (29).

## BCG induced granulocyte colony-stimulating factor, which, in turn, activated emergency granulopoiesis

The rapid increase in neutrophils suggested that BCG vaccination might induce emergency granulopoiesis (EG) (30, 31). EG is inducible after direct stimulation of hematopoietic stem cells via pattern recognition receptors (PRRs), or indirectly via reactive oxygen species (ROS) or hematopoietic growth factors (30, 31). BCG-induced EG and protection from bacterial sepsis 3 days after vaccination were observed in mice deficient in Toll-like receptor 4 (TLR4), myeloid differentiation primary response 88 (MyD88), TIR domain-containing adapter-inducing interferon-β (TRIF), S100A9, nucleotide-binding oligomerization domain (NOD), stimulator of interferon genes (STING), or Dectin, as well as in recombination-activating gene (RAG)–deficient mice, indicating that the effect did not depend on direct activation of these PRRs, their immediate downstream effectors, or V(D)J recombination (fig. S8, A to C) (32, 33). Furthermore, the ROS-mediated pathway, which can induce EG, was not required either as BCG induced neutrophil expansion in Phox-deficient mice that are unable to produce ROS (fig. S8, A to C) (29-31). Survival from neonatal sepsis was not affected by knockout of TRIF or S100A9 (fig. S8, D and E). Hematopoietic growth factors that can induce EG, such as granulocyte colony-stimulating factor (G-CSF), granulocyte macrophage-colony stimulating factor (GM-CSF), and interleukin-1β (IL-1β), IL-3, and IL-6 (30, 31) were all markedly increased within hours of BCG administration (Fig. 3A and fig. S9A). Administration of blocking or neutralizing antibodies that impaired G-CSF signaling was capable of blocking BCG-induced EG, whereas blocking any of the other EG-inducing cytokines did not affect neutrophil expansion after BCG (Fig. 3B and fig. S9B). BCG-mediated induction of EG was confirmed by up-regulation of the canonical transcriptional regulator of EG, *Cebp*-β (Fig. 3D). The lack of impact on *Cebp*-α indicated that steady-state granulopoiesis was not affected by BCG (fig. S9C) 12 hours after vaccination (30, 31). Furthermore, recombinant G-CSF (rG-CSF) administration induced BCG-like EG and also increased survival from sepsis (Fig. 3C and fig. S9D). The cytokine signal inducing EG rapidly returned to baseline 48 to 72 hours after vaccination (Fig. 1D and fig. S10). Last, EG resulted in rapid expansion of the total number of granulocyte-monocyte precursors (GMPs), as determined by culturing hematopoietic progenitors isolated from mouse spleens 2 days after vaccination in semisolid medium (Fig. 3E), as well as their in vivo expansion as determined by flow cytometry (Fig. 3F, with flow cytometry gating strategy shown in fig. S11). These data supported the hypotheses that BCG induced EG to allow rapid neutrophil expansion and that BCG-induced G-CSF was both necessary and sufficient for EG and protection.

### BCG induced EG in murine and human cohorts

To assess whether BCG vaccination induced similar mechanisms in human newborns, we measured whole-blood transcriptomes of BCG-vaccinated and unvaccinated newborns recruited in Guinea-Bissau, a low-resource setting where newborn infectious death is among the highest in the world, and compared these to BCG-induced transcriptional changes in our mouse model. We used sparse partial least squares discriminant analysis (sPLS-DA) to identify discriminatory genes between BCG-vaccinated and unvaccinated mice or humans from the multivariate feature space 24 hours after vaccination. In both cases, the identified genes separated BCG-vaccinated from unvaccinated mice (Fig. 4A) or humans (Fig. 4B). Querying the biological functions of these genes using gene set enrichment analysis (against the Broad Institute's MSigDB collection), we found that they were largely overlapping between mouse and human and specifically enriched for neutrophil function (Fig. 4C). Human findings were further validated in two independent human newborn cohorts from other low-resource settings [The Gambia and Papua New Guinea (PNG)] (Fig. 4, D and E) (34). The kinetics of BCG-induced changes of gene signatures highlight the rapid (24 hours) but short-lived (<1 week) impact of BCG on peripheral blood transcriptomics [whole-blood RNA sequencing (RNA-seq)]. Identical changes in pathways consistent with EG were detectable in all human cohorts and were limited to an early post-BCG time point. Specifically, signals reflecting G-CSF–induced changes in neutrophils were observed on day 1, but not days 3 or 7 after vaccination. Last, human newborn vaccination with BCG increased peripheral blood neutrophil counts (Fig. 4E); more specifically, BCG delayed the normal physiological contraction of the neutrophil compartment that occurs over the first week of life (35). Together, these data indicate that BCG-induced EG occurs in human and murine newborns.

## DISCUSSION

Although BCG can protect human newborns from off-target infections, possible mechanisms have thus far been investigated only in adults, and even in these adult studies, only associations have been described, not a mechanistic cause-and-effect relationship (36, 37). Our data showed that in a controlled system, BCG had nonspecific effects and reduced polymicrobial-induced septic death and bacterial burden in a neonatal mouse model via antimicrobial but not anti-inflammatory mechanisms. The ability to protect was rapid, short-lived, and dependent on BCG administration in the neonatal and juvenile, but not adult, age groups. Multiple techniques were used to identify greater neutrophil levels as both associated with improved survival and causatively linked to the ability to protect. We identified BCG-induced EG, stimulated by BCG-induced G-CSF, as both necessary and sufficient for rapid protection shortly after birth. Neutrophilic signatures were identified in both mouse and human transcriptomic data within 24 hours of vaccination, and greater neutrophil numbers were confirmed in human peripheral blood, validating a part of the mechanism in humans.

Our study has several limitations. The conclusion that BCG-induced EG was functionally responsible for the observed protection from sepsis is based on murine data only. This cannot be directly addressed in human neonates, where only associations can be inferred.

Our study focused on BCG-Denmark, but licensed BCG vaccines vary considerably in their properties (38), such that studies comparing different BCG formulations are warranted. Moreover, our human neonatal cohorts had been vaccinated with BCG and vaccines routinely recommended according to their countries' health policies [oral polio vaccine (OPV) in Guinea-Bissau, and OPV and hepatitis B vaccine in The Gambia and PNG], whereas our mice received only BCG. The other vaccines could have contributed to the observed signals in our human samples; however, our findings in murine neonates suggest that BCG was sufficient to induce EG and protection.

Given the observed longer-term protection afforded by BCG in humans, there may be additional protective pathways we did not capture in our model focused on immediate protection from sepsis (12, 13). Our study addresses BCG's nonspecific effect in the most relevant age group and setting (human newborns in low-resource settings) and focuses specifically on the most notable nonspecific protective effect of BCG, namely, the ~50% reduction in death of high-risk, low-birthweight newborns from infection within 3 days of receiving BCG (5). Neonatal susceptibility to sepsis has been linked to delayed EG (22). Increasing neutrophil numbers in the immediate newborn period may provide immediate albeit short-term protection. Although appropriately powered human newborn trial data are lacking (39), prophylactic administration of rG-CSF to newborns at risk could potentially be protective. Our findings point to opportunities to further test prophylactic interventions targeting EG in high-risk newborns.

## MATERIALS AND METHODS

### Study design

This study aimed to elucidate mechanisms responsible for nonspecific protection by BCG in early life. We had hypothesized that the ability to protect was mediated by an innate immune cell, specifically the neutrophil due to the speed of protection. Neonatal mice were used to allow for a controlled and standardized model to study relevant pathways, with survival and bacterial burden standing as measurements of disease severity. Mouse survival assays had sample size calculated as described (29). Survival assays required a minimum of 17 mice per group to detect a 40% increase in survival in mice challenged with a dose lethal for 65% of recipients ($LD_{65}$). Other assays involving a Wilcoxon rank-sum test had required group size calculated on a pilot of 10 mice using the R package "samplesize" version 0.2-4 (for both tests, an $\alpha$ error of 0.05, a $\beta$ error of 0.20, and group proportion 50:50 were used). Cytokine measurement assays had sample size selected to maximize the use of multiplex plate and standards. Flow cytometry tests analyzed by unpaired two-sided *t* test required a sample size of 5 ($\alpha$ error of 0.05 and $\beta$ error of 0.20) calculated using R package "pwr" version 1.3-0. Lung histology experiments were performed with five mice per group (40). GMP cell culturing sample size was recommended by STEMCELL Technologies. Mice were excluded if any injection leaked more than 10% or if they were a runt (greater than 25% less weight than that litter's average).

Analyzing the response to BCG in human newborns allowed us to assess whether the same signature that was functionally essential for protection from sepsis in neonatal mice was also

present in human neonates. Sample size calculations were not performed for the human experiments; instead, the maximum number of samples that were available was used.

The BCG-Immediate (BCGIMED) study inclusion criteria included informed consent, 5-min Apgar scores ≥2, and admission weight ≥ 1250 g. The exclusion criteria were gross malformations, being moribund, or prior vaccination. Inclusion criteria for The Gambia and PNG (EPIC Consortium) study sites included informed consent, a healthy-appearing infant as determined by physical examination, born by vaginal delivery at gestational age of ≥36 weeks, 5-min Apgar scores ≥8, and a birth weight ≥2.5 kg. Exclusion criteria for these sites included any positive screening results for maternal HIV-1 and HIV-2 and hepatitis B. BCGIMED was randomized, whereas The Gambia and PNG sites recruited participants as part of an observational study assessing the impact of standard local immunization recommendations.

For work involving both mice and humans, the experimental end points were predetermined. Most mouse experiments were not blinded but were anonymized by mouse number after treatment and were split evenly by sex between treatment groups, followed by randomization. An exception to this was the histological scoring of mouse lungs for inflammatory damage, where the pathologists were not informed of group status, treatment, or the hypotheses of the study and were only tasked with scoring for inflammatory markers and neutrophil status. Those administering the vaccine to human neonates were not blinded to subject treatment status, but the subsequent blood draw and performance of techniques like flow cytometry were blinded to treatment.

### Mice and monitoring

All animal work conducted was approved by the Institutional Animal Care and Use Committee at the University of British Columbia (UBC) (protocol A17-0110). Specific pathogen–free male and female mouse breeding pairs for C57BL/6J (B6, stock number 000664) and knockouts for *RAG-1* (stock number 002216)–, *Dectin-1* (stock number 012337)–, *TRIF* (stock number 005037)–, *NOD-2* (stock number 005763)–, *gp91phox* (Phox/ROS, stock number 002365)–, *STING* (stock number 025805)–, and *GM-CSF* (stock number 026812)–deficient (homozygous) mice (all on a C57BL/6J background) were purchased from The Jackson Laboratory. *MyD88*-deficient mice [B6.129P2(SJL)-*Myd88*$^{tm1.1Defr}$/J] were a gift from B. Vallance (UBC), *TLR4* knockout mice were a gift from B. Verchere (UBC), *G-CSF* knockout mice were a gift from M. Hibbs (Ludwig Institute for Cancer Research), and *S100A9* were a gift from T. Vogel (Institute of Immunology, Muenster, Germany). All mice were allowed 7 days to adjust to their new environment before breeding was initiated at 6 to 10 weeks of age. Nonbreeding mice were maintained on standard rodent food (Teklad, 2918), whereas breeding mice were on a high-fat diet (Teklad, 2919), and both had water ad libitum. To generate neonatal mice, paired matings were established twice weekly; females were isolated from males as soon as they were visually identified as pregnant and followed twice daily thereafter to record an accurate date of birth.

### Murine BCG vaccination

Lyophilized BCG (Danish strain 1331) from Statens Serum Institute, Denmark, was stored at −80°C until reconstitution with 1 ml of Sauton serum. Vials were inverted three to five times, then gently mixed three times with a 28-gauge syringe, and stored at 4°C until injection. Mice were vaccinated on DOL 4 to 5 via a 50-μl subcutaneous injection of $1 \times 10^5$ to $4 \times 10^5$ colony-forming units (CFU) as per product insert sheet and as published (41-43). Mice vaccinated during the juvenile and adult age frames (DOL 21 and 6 weeks of age, respectively) were subcutaneously administered an adult dose of $2 \times 10^5$ to $8 \times 10^5$ BCG CFU in 100 μl.

### Murine sepsis challenge

The neonatal sepsis mouse model was performed as previously described (18, 19, 29). Briefly, CS was obtained from adult (aged 6 to 12 weeks) male caeca and resuspended in dextrose 5% water (D5W; Baxter, JB0081) at a concentration of 160 mg CS/ml D5W and then passed through a 70-μm filter (Falcon, 352350). Aliquots were divided and frozen at −80°C until challenge. Storage at −80°C had no effect on CS viability over 6 months (29). Aliquots were thawed and diluted further with D5W, and neonatal mice at DOL 7 (3 days after vaccination) were challenged via intraperitoneal injection of 100 μl of CS at a litter- and weight-adjusted dose as described (29). Before challenge, a working stock was prepared on the basis of the average weight of the litter. Individual doses were then adjusted through multiplying the average dose by each mouse's percent weight difference compared with that litter's average weight. For mice that received BCG vaccination as neonates and had challenge delayed to the juvenile period, challenge commenced on DOL 14 to 17. For mice that received BCG vaccination as juvenile mice at DOL 18, challenge commenced on DOL 21. Adult mice vaccinated at 6 weeks were challenged 3 days later. To account for batch and potential donor variation, each preparation of CS was titered in control mice to reach an LD as desired for a given experiment. This specific, weight-adjusted dose ranged from 0.80 to 0.95 mg CS/g mouse, depending on the desired LD, mouse strain, and batch effects. The same batch of CS and challenge dose was kept constant for an entire experiment. Litter-to-litter variation was accounted for by having a balanced number of treated and control mice in each litter.

### Murine LPS challenge

Neonatal mice were intraperitoneally challenged with a dose of LPS (from *Escherichia coli* O26:B6, Sigma, L8274) pretitered to yield an $LD_{70}$. Administration was in a weight-adjusted dose. The stock was diluted in endotoxin-free Dulbecco's phosphate-buffered saline (dPBS) (Gibco, catalog no. 14190-144) with the average mouse receiving 15 μg LPS/g body weight in a 100-μl injection. This strategy allowed for injection volumes and dosages of LPS to be similar between litters that varied in weight.

### Murine monitoring and humane end point

Mice were monitored as in (29). Briefly, mice were monitored 2 hours after challenge and then every 4 to 6 hours over the first 2 days, followed by monitoring one to two times per day and with increased frequency if mice displayed declining health. Humane end point was

determined using righting reflex and mobility, as previously described (29). Juvenile and adult mice that were challenged were observed as described in table S2.

### Quantifying bacterial burden in mice

After euthanasia with isoflurane and $CO_2$, blood was slowly drawn via cardiac puncture into a 28-gauge insulin syringe (BD, 329461) preloaded with 10 μl of heparin (1000 U/ml; Fresenius Kabi Canada, DIN 02264307) and placed on ice. Peritoneal wash was obtained by intraperitoneally injecting 500 μl of sterile dPBS (Gibco, catalog no. 14190-144) and then gently massaging the body cavity 20 times before aseptic aspiration. Organs were dissected with tools sterilized by hot-bead sterilizer, and organs were placed into preweighed microcentrifuge tubes (spleen) or 15-ml Falcon tubes (liver and lung), weighed, and held on ice. The spleen was homogenized by being pushed through a 70-μm filter placed in a 35-mm petri dish using the plunger of a 1-ml syringe (BD, 1187A16). The liver and lung were homogenized using a handheld homogenizer (Polytron, PT 1200 E). Each organ was serially diluted 1:10 (up to $10^6$), and 40 μl of each dilution was plated on 5% sheep blood agar plates (sheep blood, Dalynn, HS30; tryptic soy agar, Sigma, 22091). Bacterial CFU were counted after 18- to 22-hour incubation at 37°C. For solid organs, bacterial burden was represented per gram tissue to account for differences in organ and mouse sizes.

### Adoptive transfer of splenocytes between mice

Neonatal spleens containing immune and hematopoietic progenitor cells were adoptively transferred by an intraperitoneal injection of 50 μl of cell suspension or a control injection of dPBS followed immediately by the injection of 100 μl of CS previously titered to an $LD_{70}$ into the same compartment to induce sepsis. The cells were collected from age- and sex-matched control or BCG-vaccinated donor spleens 3 days after vaccination. Spleens were disrupted as previously described, placed in endotoxin-free dPBS and cryovials (Corning, 430658), and stored at room temperature (RT) without red blood cell (RBC) lysis (44). Tissues from multiple age-matched and sex-matched donors were combined into a single 70-μm cell strainer, gently dissociated through the filter using the plunger of a 1-ml syringe, centrifuged for 5 min at 470*g*, and counted using an automated cell counter and dye (Nexcelom Bioscience Cellometer Auto 2000, ViaStain CS2-0106). The cells at this stage were used in the three experimental setups shown in fig. S4: (i) adoptive transfer of the heterogeneous whole-spleen compartment, (ii) depletion of mature neutrophils via biotin anti-Ly6G and magnetic anti-biotin separation (Miltenyi, 130-107-911 and 130-097-046), or (iii) neutrophil purification by negative magnetic selection (Miltenyi, 130-097-658). These selection procedures were performed according to the manufacturer's recommendations, with the exception that processes were performed at RT and without RBC lysis. The number of viable cells adoptively transferred was based on the average number of cells found within the spleen of a 7- to 8-day-old mouse ($4 \times 10^6$ cells/g mouse for the whole spleen). Mature neutrophils accounted for 5% of the whole-spleen cellular compartment; therefore, $2 \times 10^5$ neutrophils/g mouse were transferred in the purified neutrophil experiment. Control neutrophils were also purified and scaled up beyond the number in a normal control spleen so that the number of neutrophils would be the same as in the BCG-vaccinated donors. In the depletion experiment, the number of cells transferred was adjusted for the removal of the neutrophil population, and $3.85 \times 10^6$ cells/g mouse were transferred to recipient neonatal

mice. An aliquot of each purification or depletion sample was assessed by flow cytometry using the neutrophil markers CD11b$^{pos}$, Ly6G$^{hi}$, Ly6C$^{int}$, CD3$^{neg}$, MHCII$^{neg}$, and NK1.1$^{neg}$, as described (45), to verify purity, which was consistently >95%.

### Murine plasma cytokine production

After isoflurane and $CO_2$ euthanasia, blood was promptly obtained via cardiac puncture with a 28-gauge insulin syringe preloaded with 10 μl of heparin (1000 U/ml). Blood was stored on ice for up to 30 min and centrifuged with soft brake at 650*g* for 10 min. Plasma was then collected and stored at −80°C for further quantification of plasma cytokines and chemokines. Murine plasma was used to measure cytokine concentrations using a predesigned Multi-Analyte Cytokine Mouse Magnetic Panel bead array (Thermo Fisher Scientific, EPX480-20834-901) following the manufacturer's recommendations. The panel detected the following 47 analytes: B cell activating factor (BAFF), betacellulin (BTC), epithelial-derived neutrophil-activating peptide 78 (ENA-78), Eotaxin, G-CSF, GM-CSF, growth-regulated oncogene-α (GRO-α), interferon-α (IFN-α), IFN-γ, IL-12p70, IL-10, IL-13, IL-15, IL-17A, IL-18, IL-19, IL-1α, IL-1β, IL-2, IL-22, IL-23, IL-25, IL-27, IL-28, IL-2RA, IL-3, IL-31, IL-33, IL-33R, IL-4, IL-5, IL-6, IL-7, IL7-RA, IL-9, interferon gamma-induced protein 10 (IP-10), Leptin, monocyte chemoattractant protein-1 (MCP-1), MCP-3, M-CSF, macrophage inflammatory protein-α (MIP-1α), MIP-1β, MIP-2, receptor activator of nuclear factor kappa B ligand (RANKL), regulated on activation, normal T cell expressed and secreted (RANTES), tumor necrosis factor-α (TNF-α), and vascular endothelial growth factor A (VEGF-A). Results were obtained with a FLEXMAP 3D System (CS1000) with MasterPlex CT version 1.2.0.7 (Hitachi Solutions America). Cytokine concentrations were determined using R (version 3.4.3) and "drLumi" (version 0.1.2).

### Inhibition of EG-inducing cytokines

Cytokines previously reported to be able to induce EG (30, 31) were inhibited by injection of antibody or biological inhibitors. Anakinra [Kineret from Sobi DIN 02245913; anti-IL-1 at 25 μg/g mouse as used in (46)], etanercept [Enbrel from Amgen, DIN 02242903; anti–TNF-α at 15 μg/g mouse as used in (47)], tocilizumab [Actemra from Roche, DIN 02350092; anti-IL-6R at 5 μg/g mouse as used in (48)], anti–IL-3 (aIL3 from Abcam, ab9726; at 2.5 μg/g mouse as recommended by the product sheet], anti–G-CSF (from R&D Systems, MAB414; 10 μg per injection as used in (49)], and anti–GM-CSF (from Abcam, ab9741; at 10 μg/g mouse as recommended by the product sheet] were each administered in 40-μl intraperitoneal doses to separate mice 12 hours before vaccination, at vaccination, and at 24 and 48 hours after vaccination until euthanasia at 72 hours after vaccination for flow cytometry of splenocytes.

### rG-CSF administration

Neonatal mice were administered rG-CSF in lieu of BCG vaccination on DOL 4 to 5. These mice were then followed until 3 days after vaccination for flow cytometry of splenocytes or challenged with CS and followed for survival. rG-CSF was tested in a dose-titration flow cytometry experiment with an intraperitoneal injection volume of 40 μl and a range of doses from 10 μg of rG-CSF/g mouse to 0.001 μg/g before the mortality experiment.

### TaqMan real-time polymerase chain reaction

RNA samples were collected from mouse spleens 12, 24, and 36 hours after vaccination. Spleens were harvested as previously described and immediately placed into 1 ml of RNAlater (Invitrogen, AM7020), held at 4°C for 24 hours to allow tissue perfusion, and stored at −80°C. Before extraction, spleens were moved to RNAlater-ICE transition solution (Invitrogen, AM7030) and held at −20°C for 24 hours as per the manufacturer's instructions. RNA was extracted following the manufacturer's protocol (QIAGEN, 74034), followed by reverse transcription using the high-capacity complementary DNA (cDNA) reverse transcription kit (Thermo Fisher Scientific, catalog no. 4374966) as per the manufacturer's recommendations, and amplified on a Biometra TGradient. Up to 100 ng of cDNA was used to run the real-time quantitative polymerase chain reaction (PCR) with the TaqMan Fast Advanced Master Mix Kit with ROS passive reference dye (Thermo Fisher Scientific, catalog no. 4444557). The cDNA amplification was performed on the ViiA 7 System thermocycler (Applied Biosystems), and data were collected from the device using the ViiA 7 software. The following primer sequences were used to quantify the expression of the *Cebp*-β gene and the *Cebp*-α gene: *Cebp*-β gene, 5′-AAGCTGAGCGACGAGTACAAGA-3′ (forward) and 5′-GTCAGCTCCAGCACCTTGTG-3′ (reverse); *Cebp*-α gene, 5′-AAAGCCAAGAAGTCGGTGGAC-3′ (forward) and 5′-CTTTATCTCGGCTCTTGCGC-3′ (reverse). Unlabeled primers were purchased from Integrated DNA Technologies. The mouse housekeeping gene primers and probe were predesigned and validated by Thermo Fisher Scientific (18*S*, Hs99999901_s1, catalog no. 4448484). The reporter gene probe had 5′VIC and a minor groove binder (MGB) quencher. The probes used for *Cebp*-β and *Cebp*-α were designed with a 5′FAM and a 3′QSY quencher to be run in duplex with the housekeeping gene, but in separate wells from each other. The sequence of the probe for *Cebp*-β was 5′-CGAGCGCAACAACATCGCGG-3′, whereas the probe sequence for *Cebp*-α was 5′-CGAGTACCGGGTACGGCGGGAAC-3′. The probes were purchased from Life Technologies, high-performance liquid chromatography purified, and complexed in-house with the unlabeled primers at a final concentration of 5 μM for probe and 18 μM for primers. Each cDNA sample was run in triplicate.

### Flow cytometry

Spleen samples were collected and counted as described above for adoptive transfer of splenocytes between mice. To stain the neutrophils, 1.5 to 2 million total whole-spleen cells were resuspended in 100 μl of sterile dPBS with 0.1 μl of viability dye (eBioscience, catalog no. 65-0866-14), incubated for 30 min at RT, and resuspended in 100-μl Smart Lyse (Smart Tube Inc., catalog no. 3T5070) and 350-μl Smart Store (Smart Tube Inc., catalog no. STBLSTORE2-1000) before being frozen at −80°C. On the day of the assay, fixed cells were thawed at 10°C, centrifuged for 5 min at 600*g*, and resuspended with a staining cocktail solution containing antibodies specific to major histocompatibility complex II (MHCII) (clone M5/114.15.2; eBioscience, 47-5321-82), CD11b (clone M1/70; eBioscience, 17-0112-82), F4/80 (clone BM8; eBioscience, 25-4801-82), NK1.1 (clone PK136; BD, 557391), CD3 (clone 17A2; eBioscience, 46-0032-80), CD11c (clone N418; BioLegend, 117339), Ly6C (clone AL-21; BD, 563011), and Ly6G (clone RB6-8C5;

eBioscience, 48-5931-82). Cells were stained at RT for 45 min and washed twice with PBSAN [dPBS with 10% sodium azide and 5% bovine serum albumin (BSA)].

Samples for progenitor assessment were processed fresh. First, the whole-spleen cells were homogenized and resuspended in dPBS mixed with viability dye and anti-CD16/32 (clone 2.4G2; BD, 563006). The cells were incubated for 30 min at 4°C. Cells were then washed once with PBSAN, then resuspended in PBSAN with anti-CD34 (clone RAM34; eBioscience, 56-0341-82), and stained for 1 hour at 4°C. Without washing, a cocktail of antibodies against CD117 (clone 2B8; eBioscience, 17-1171-83), CD135 (clone A2F10; eBioscience, 12-1351-83), Ly6A/E (clone D7; eBioscience, 11-5981-85), and the lineage markers Ter-119 (clone Ter-119; eBioscience, 13-5921-75), CD11b (clone M1/70; eBioscience, 13-0112-75), CD3e (clone 145-2C11; eBioscience, 13-0031-75), Ly6G (clone RB6-8C5; eBioscience, 13-5931-75), and CD45R (clone RA3-6B2; eBioscience, 13-0452-75) were added. Cells were stained for 30 min at RT. Last, the cells were washed with PBS, resuspended with streptavidin (BD, 563858), incubated for 20 min at RT, and then washed with PBSAN.

Flow cytometric acquisition used a custom-built BD LSRII. Mature neutrophils were identified as $CD11b^{pos}$, $Ly6G^{hi}$, $Ly6C^{int}$, $CD3^{neg}$, and $MHCII^{neg}$, $NK1.1^{neg}$, and immature neutrophils as $CD11b^{pos}$, $Ly6G^{int}$, $Ly6C^{int}$, $CD3^{neg}$, $MHCII^{neg}$, and $NK1.1^{neg}$, as described (45). GMP progenitor cells were identified as in (50) as live cells, $Lin^{neg}$, $CD117^{pos}$, $Ly6A/E^{neg}$, $CD16/32^{pos}$, and $CD34^{pos}$.

## STEMCELL culturing of progenitor populations

Neonatal mouse spleens were collected and dissociated in sterile and endotoxin-free conditions through the same technique used in the adoptive transfer above. The cells were stored in Iscove's modified Dulbecco's medium with 2% fetal bovine serum (STEMCELL Technologies, 07700) on ice and delivered to STEMCELL Technologies (Vancouver, BC) for culture of cells at $1 \times 10^5$ cells per well in a semisolid medium, MethoCult (M3234), supplemented with recombinant mouse G-CSF (100 ng/ml) and recombinant mouse GM-CSF (10 ng/ml), with colonies counted after 7 days of culture by researchers blinded to treatment.

## Mouse whole-blood RNA extraction

Control and BCG-vaccinated mice were euthanized, and whole blood was immediately drawn via cardiac puncture using a 28-gauge needle into a syringe preloaded with 10 μl of sodium heparin at 1000 U/ml placed in 2.0-ml cryovials preloaded with 1.3 ml of RNAlater (Invitrogen, AM7020) and stored at −80°C until RNA extraction. Total RNA was extracted from up to 150 μl of RNAlater-preserved whole mouse blood using the Ambion RiboPure Human Blood Kit (Ambion, Thermo Fisher Scientific, AM1928) with the following modifications to the manufacturer's extractions: For step 1 of the cell lysis and initial RNA purification protocol, once thawed at RT, whole-blood samples were transferred to 2-ml RNase-free tubes and centrifuged for 3 min at 14,000 rpm. For step 3, after the addition of 500 μl of acid phenol-chloroform and incubation at RT, the samples were centrifuged at 3200 rpm for 10 min. The remainder of the steps were followed as per the manufacturer's

protocol and included the optional deoxyribonuclease I treatment. Quantification and quality assessment of total RNA used an Agilent 2100 Bioanalyzer.

## Lung histology and scoring

Neonatal mice that were vaccinated on DOL 4 to 5 and CS challenged 3 days later were euthanized for lung histology 24 hours after challenge. After isoflurane-induced euthanasia, the mice were checked for automatic reflexes, and the chest cavity was exposed. The muscles around the neck were carefully moved away, and the sternum was separated, revealing the trachea and lungs. A catheter was inserted into the trachea, and the lungs were filled with 10% buffered formalin with a reservoir at 14 inches, 35.5 cm above the chest of the mouse prior to the trachea being securely tied and the lungs placed into 10% buffered formalin. After fixation for 24 to 48 hours at RT, formalin was replaced with 70% ethanol, after which the lungs were dehydrated, paraffin embedded, and longitudinally sectioned to 5 μm along the main axial airway. Hematoxylin and eosin and Ly6G staining was performed on separate but serial sections, and scoring by trained pathologists was performed blinded to treatment group and to study hypotheses. Scoring of sections involved observation of alveolar damage, alveolar monocyte count, perivascular cuffing, reactive bronchial cells, peribronchial cuffing, lung expansion, neutrophil recruitment (with higher score meaning more neutrophils), and inflammation score.

## Human sample collection and analysis

Human newborn samples were collected from two different studies covering three different populations: the BCGIMED study at the Bandim Health Project in Guinea-Bissau and the EPIC-Human Immune Project Consortium (EPIC-HIPC) in both PNG (Institute of Medical Research) and The Gambia Medical Research Council, with coordination of sample and data flow for EPIC-HIPC via the Precision Vaccines Program Clinical and Data Management Cores at Boston Children’s Hospital. All studies were approved by the University of British Columbia ethics board (protocol nos. H14-03369 and H16-02409). In addition, each site involved had obtained ethics approval from the Ethical Committees in their respective country of research. Informed consent was obtained from the parents/guardians at the time of the recruitment to the studies, and the studies were conducted in accordance with the Helsinki Declaration ethical standards.

## The BCGIMED study

Samples collected from Guinea-Bissau were auxiliary to the BCGIMED study (clinical trial registration number NCT01989026), where newborns admitted to the neonatal nursery at the tertiary care center Hospital National Simao Mendes were randomized to receive BCG-Danish Strain 1331 (Statens Serum Institute) and OPV either at birth or at hospital discharge as per regular practice for newborns admitted to nursery care. Capillary blood was collected via heel-prick from the newborns 24 hours after randomization, when half of newborns had received the vaccines and half were unvaccinated.

### BCGIMED peripheral blood processing

Capillary blood (400 μl) was collected into lithium-heparin microtainers (BD, catalog no. 365965) via heel-prick blood draw. Aliquots (200 μl) were immediately placed into 1.3 ml of RNAlater (Invitrogen, AM7020) and stored at −80°C within 3 hours of blood draw until further analysis. Samples were subsequently ground transported to the Medical Research Council (Gambia) on dry ice by the study personnel and then to the UBC (Vancouver, British Columbia, Canada) under temperature-controlled and monitored conditions (World Courier).

### BCGIMED whole-blood RNA extraction

Total RNA was extracted from each sample using the Human RiboPure RNA Purification Kit (Ambion, Thermo Fisher Scientific, AM1928) following the manufacturer's protocol. Quantification and quality assessment of total RNA were performed using an Agilent 2100 Bioanalyzer.

### The EPIC study

This study is registered under clinical trials no. NCT03246230. In the Gambia and PNG (EPIC Consortium study sites), the nonvaccinated control group had samples obtained before DOL 7 administration of BCG-Russia, OPV, and Hepatitis B vaccine (all from Serum Institute of India) as per local standard of care [see (34)]. The treatment group of newborns received BCG, OPV, and hepatitis B vaccine at birth. Peripheral blood samples were obtained from all infants on the day of birth, and one additional sample was then collected at day 1, 3, or 7 after vaccination to reduce venipunctures to a maximum of two within the first week of life. This allowed contrasting of vaccinated versus unvaccinated newborns over the first week of life (34).

### EPIC peripheral blood processing

Venous blood was collected directly into 4-ml preheparinized collection tubes (75 United States Pharmacopeia (USP); VWR, catalog no. 367871) by the "drip-blood" collection method until 2 ml was collected. Aliquots (~200 μl) were immediately placed in RNAlater (Invitrogen, AM7020) with the remaining blood kept in the collection tubes at RT until further processing within 4 hours. Whole blood was centrifuged on site at 500*g* for 10 min at RT, and plasma was removed. The amount of plasma removed from the whole blood after centrifugation was subsequently replaced with RPMI. For later assessment of cellular composition by flow cytometry, EDTA (0.2 mM final concentration; Invitrogen, catalog no. 15575-038) was added to the whole blood/RPMI mixture to ensure adherent cells were not lost. Blood sample aliquots (225 μl) were stained for viability with 2 μl of fixable viability dye (eBioscience, catalog no. 65-0865-14) for 30 min at 4°C in the dark, RBCs were lysed and cells were fixed in 350 μl of Stable-Lyse V2 buffer (Smart Tube Inc., catalog no. STBLYSE2-250) for 15 min at RT, and then 1 ml of Stable-Store V2 (Smart Tube Inc., catalog no. STBLSTORE2-250) was added and incubated for 15 min at RT before storage at −80°C. Samples were subsequently shipped to UBC under temperature-controlled and monitored conditions (World Courier).

### Transcriptomic analysis of mouse and human-BCGIMED whole-blood RNA

mRNA from mouse and human (BCGIMED study, Guinea-Bissau) whole-blood RNA extracts were measured using the nCounter Immunology Profiling Panels (NanoString Technologies), applying 100 ng of total RNA from each sample. RNA profiling was performed according to the manufacturer's instructions (high-sensitivity setting), and flow cartridges were read on the nCounter FLEX digital imaging system (maximum fields of view setting). Mouse and human data were processed separately. Reporter code count (RCC) files were normalized using sample-specific normalization factors calculated with probe set–specific housekeeping gene counts. ComBat batch correction (51) was used to normalize across multiple cartridges. Batch-corrected data were $\log_2$ transformed. sPLS-DA (52) was used to identify discriminatory genes for vaccination status. Mouse and human models were constructed using two components with 60 genes (mouse) and 100 genes (BCGIMED) per component. Genes selected by sPLS-DA were compared to a series of cell-specific gene signatures derived from (53). Signatures were assessed for overrepresentation in the sPLS-DA–selected genes using Fisher's exact test.

### EPIC-human flow cytometry

At the immunophenotyping laboratory, flow cytometry samples were thawed, washed in staining buffer (PBSAN: 0.5% BSA and 0.1% sodium azide), and stained on ice in PBSAN with a cocktail of anchor markers to determine the frequency and the absolute counts of neutrophils in peripheral blood as previously described (34). Raw values were normalized with a $1 + \log_2$ transformation. To account for interindividual fluctuations of circulating cell counts, each sample was indexed to its corresponding subject's prevaccination cell counts using a withinVariation matrix by the withinVar function in R package "mixOmics" (version 6.1.2). Normalized neutrophil counts were compared between vaccinated and unvaccinated samples separately for each postvaccination DOL using the Wilcoxon rank-sum test.

### RNA-seq profiling of human-EPIC whole-blood RNA

Total RNA was extracted from each sample, and strand-specific cDNA libraries were generated from poly-adenylated RNA, as previously described (34). All cDNA libraries were prepared at the same time and sequenced on the HiSeq 2500 (Illumina). Reads were aligned to the hg38 human genome (Ensembl GRCh38.86) using STAR v2.5 and mapped to Ensembl GRCh38 transcripts. Read counts were generated using htseq-count (HTSeq, 0.6.1p1). Globin transcripts were removed in silico. Genes with very low counts (less than 10 counts in eight or more samples or the smallest number of biological replicates within each treatment group) were discarded. Counts were normalized to library size using total count normalization and $\log_2$ transformed. Transcript-level count data were summarized to gene level by averaging. We further decomposed the within-subject from the between-subject variance in the datasets using mixOmics' withinVar function to account for repeated measures (day 0 or day 1, 3, or 7 after vaccination). We then searched the Broad Institute's Molecular Signatures Database (MSigDB) immunologic gene set collection (C7) (54) for signatures of growth factor–induced changes in neutrophils, indicating possible EG signatures, and found six such gene sets:
GSE15139_GMCSF_TREATED_VS_UNTREATED_NEUTROPHILS_DN,

GSE15139_GMCSF_TREATED_VS_UNTREATED_NEUTROPHILS_UP, GSE22103_LPS_VS_GMCSF_AND_IFNG_STIM_NEUTROPHIL_DN, GSE22103_LPS_VS_GMCSF_AND_IFNG_STIM_NEUTROPHIL_UP, GSE22103_UNSTIM_VS_GMCSF_AND_IFNG_STIM_NEUTROPHIL_DN, and GSE22103_UNSTIM_VS_GMCSF_AND_IFNG_STIM_NEUTROPHIL_UP.

Gene sets corresponding to up- and down-regulated gene lists for equivalent perturbation experiments were combined. We next assessed the ability of each of the three resulting neutrophil-specific, EG-related signatures to separate vaccinated from unvaccinated samples in the EPIC RNA-seq data by carrying out PCA using these subsets of genes. This was done using EPIC data from all DOLs jointly. PCA variates were then separated by DOL and the distinctness of the clusters formed by vaccinated and unvaccinated samples was tested using PERMANOVA.

### Statistical analysis

Survival after polymicrobial sepsis and endotoxemia was determined as previously described (29). Briefly, survival curves were compared between groups using a log-rank test. Data were tested for normality either by using the Shapiro-Wilk test, rejecting the null hypothesis when $P < 0.1$, or through visual inspection of qqplot and distribution. Cytokine concentrations, neutrophil flow cytometry, progenitor flow cytometry, PCR results, and STEMCELL-cultured progenitor cells were compared using the Student's $t$ test applied at each time point assessed [with Benjamini-Hochberg (BH) adjustment for multiple comparisons where applicable]. To further test hypotheses that BCG vaccination increased neutrophil numbers and decreased bacterial load after the primary observation, one-tailed tests were applied. Measurements that failed normality tests (bacterial load in blood, peritoneal wash, and organs) were analyzed with Wilcoxon rank-sum tests (BH adjusted when appropriate) or a Kruskal-Wallis rank-sum test before post hoc pairwise comparisons within treatments using the Wilcoxon rank-sum test. Differences were considered significant with $P < 0.05$, and exact $P$ values or different thresholds of $P$ values were presented in each figure legend. Boxplots were presented as median with 25 to 75% interquartile range (IQR), and cytokine data as mean ± SEM. PCA was used to visualize global plasma cytokine responses at various time points after vaccination using $\log_2$ transformed cytokine values. R (version 3.5.4) was used to perform the analyses.

## Supplementary Material

Refer to Web version on PubMed Central for supplementary material.

## Acknowledgments:

We would like to thank all the participants and their parents for the time and willingness to support this study. We also want to thank C. Harrison and the staff at the animal care facility at British Columbia Children's Hospital Research Institute. We extend our thanks to students and volunteers who have helped over the years, specifically to D. Zhao, K. Elward, J. Mao, R. Zhong, M. Yerrabattini, A. Roshan, C. Sutton, M. Tan, M. Xu, I. Jankowski, G. Gill, E. Ssebuliba, S. Dunehav, and L. Bergqvist. We would also like to acknowledge B. Vallance, B. Verchere, T. Vogel, and M. Hibbs for the gifts of mouse knockout strains. The G-CSF and S100A9 mouse knockout strains were from M. Hibbs (Ludwig Institute for Cancer Research) and T. Vogel (Institute of Immunology, Muenster, Germany), respectively. We also thank A. Oznoff and J. Arce of the Precision Vaccines Data Management Core (Boston Children's Hospital) for expert assistance with data management, D. Vo and K. Kraft of the Precision

Vaccines Program for the administrative and organizational assistance, and G. Fleisher, M. Wessels, and D. Kim of Boston Children's Hospital for the support.

**Funding:** This work was in part supported by the National Institute of Allergy and Infectious Diseases (NIAID) of the NIH as part of the Human Immunology Project Consortium under 5U19AI118608-02. The content is solely the responsibility of the authors and does not necessarily represent the official views of the NIH. T.K.'s laboratory was supported by Telethon Kids and the Perth Children's Hospital Foundation, as well as a Michael Smith Foundation for Health Research Career Investigator Award. The Precision Vaccines Laboratory (directed by O.L.) is supported by the following U.S. NIH/NIAID awards: Molecular Mechanisms of Combination Adjuvants (1U01AI124284-01), Adjuvant Discovery Program (contract no. HHSN272201400052C), Adjuvant Development Program (contract no. HHSN272201800047C), and an internal Boston Children's Hospital award. B.K. is supported by funding from the Medical Research Council, UK (MR/R005990/1 and MC_UP_A900/1122, MC_UP_A900/115). J.L.W. is supported by NIH/NICHD (R01HD089939 and R01HD097081) and NIH/NIGMS (R01GM128452). The BCGIMED study was supported by CVIVA and the Danish National Research Foundation (DNRF108), as well as the Karen Elise Jensens Fond, the Augustinusfonden, Else og Mogens Wedell Wedellborgs Fond, and the Fonden til Lægevidenskabens Fremme.

## Appendix

## The Expanded Program on Immunization (EPIC) Consortium:

In addition to EPIC Consortium members who are authors (Danny Harbeson, Casey Shannon, Rym Ben-Othman, Bing Cai, Daniel He, Ofer Levy, Beate Kampmann, Scott Tebbutt, Nelly Amenyogbe, and Tobias Kollmann), the following EPIC Consortium members are collaborators who have contributed to the collection and analysis of human samples and data from The Gambia and Papua New Guinea presented in this manuscript:

Amy H. Lee[19], Tue B. Bennikeyy[20], Joann Diray-Arce[9,10], Olubukola Idoko[12,21], William S. Pomat[22], Simon van Haren[9,10], Momoudou Cox[12], Alansana Darboe[12], Reza Falsafi[19], Samuel H. Hinshaw[19,23], Jorjoh Ndure[12], Jainaba Njie-Jobe[12], Matthew A. Pettengill[24], Arnaud Marchant[25], Peter C. Richmond[26,27], Rebecca Ford[22], Gerard Saleu[22], Geraldine Masiria[22], John Paul Matlam[22], Wendy Kirarock[22], Elishia Roberts[12], Mehrnoush Malek[28], Guzman Sanchez-Schmitz[9], Amrit Singh[29], Asimenia Angelidou[9,30], Kinga K. Smolen[9,10], Ryan R. Brinkman[28], Al Ozonoff[9,10], Robert E.W. Hancock[19], Anita H.J. van den Biggelaar[27], Hanno Steen[9,31], Diana Vo[9], Ken Kraft[9], Kerry McEnaney[9], Sofia Vignolo[9].

[19]Department of Microbiology and Immunology, University of British Columbia, 1365-2350 Health Sciences Mall, Vancouver, BC V6T 1Z3, Canada. [20]Department of Health Science and Technology, Aalborg University, Fredrik Bajers Vej 7 D2, 9220 Aalborg, Denmark. [21]Center for International Health, Medical Center of the University of Munich (LMU), 80539 Munich, Germany. [22]Papua New Guinea Institute of Medical Research, Homate Street, 441 Goroka, Eastern Highlands Province, Papua New Guinea. [23]Graduate Program in Bioinformatics, BCCA, 100-570 West 7th Avenue, Vancouver, BC V5Z 4S6, Canada. [24]Department of Pathology, Anatomy and Cell Biology, Thomas Jefferson University, Jefferson Alumni Hall, 1020 Locust Street, Suite 279, Philadelphia, PA 19107, USA. [25]Institute for Medical Immunology, Université libre de Bruxelles, Charleroi, Rue Adrienne Bolland 8, 6041 Gosselies, Belgium. [26]Division of Paediatrics, School of Medicine, University of Western Australia, 35 Stirling Highway, Nedlands, WA 6009, Australia. [27]Wesfarmers Centre of Vaccines and Infectious Diseases, Telethon Kids Institute, University of Western Australia Perth, 15 Hospital Avenue, Nedlands, WA 6009, Australia. [28]BC Cancer Agency, 686 West Broadway, Suite 500, Vancouver, BC V5Z 1G1, Canada.

[29]Department of Pathology and Laboratory Medicine, Faculty of Medicine, University of British Columbia, Rm. G227–2211 Wesbrook Mall, Vancouver, BC V6T 2B5, Canada. [30]Division of Newborn Medicine, Boston Children's Hospital, 300 Longwood Ave., BCH 3146, Boston, MA 02115, USA. [31]Department of Pathology, Boston Children's Hospital, BCH 3108, 300 Longwood Ave., Boston, MA 02115, USA.

## REFERENCES AND NOTES

1. U. N. C. s. Fund, in U.N. Data, U.N., Ed. (U.N., Geneva, 2019).
2. Shane AL, Stoll BJ, Neonatal sepsis: Progress towards improved outcomes. J. Infect 68 (Suppl. 1), S24–S32 (2014). [PubMed: 24140138]
3. Santos RP, Tristram D, A practical guide to the diagnosis, treatment, and prevention of neonatal infections. Pediatr. Clin. North Am 62, 491–508 (2015). [PubMed: 25836710]
4. Lawn JE, Blencowe H, Oza S, You D, Lee AC, Waiswa P, Lalli M, Bhutta Z, Barros AJ, Christian P, Mathers C, Cousens SN, Every newborn: Progress, priorities, and potential beyond survival. Lancet 384, 189–205 (2014). [PubMed: 24853593]
5. Seale AC, Blencowe H, Manu AA, Nair H, Bahl R, Qazi SA, Zaidi AK, Berkley JA, Cousens SN, Lawn JE, Estimates of possible severe bacterial infection in neonates in sub-Saharan Africa, south Asia, and Latin America for 2012: A systematic review and meta-analysis. Lancet Infect. Dis 14, 731–741 (2014). [PubMed: 24974250]
6. Schaltz-Buchholzer F, Biering-Sorensen S, Lund N, Monteiro I, Umbasse P, Fisker AB, Andersen A, Rodrigues A, Aaby P, Benn CS, Early BCG vaccination, hospitalizations, and hospital deaths: Analysis of a secondary outcome in 3 randomized trials from Guinea-Bissau. J. Infect. Dis 219, 624–632 (2019). [PubMed: 30239767]
7. Okomo U, Akpalu ENK, Le Doare K, Roca A, Cousens S, Jarde A, Sharland M, Kampmann B, Lawn JE, Aetiology of invasive bacterial infection and antimicrobial resistance in neonates in sub-Saharan Africa: A systematic review and meta-analysis in line with the STROBE-NI reporting guidelines. Lancet Infect. Dis 19, 1219–1234 (2019). [PubMed: 31522858]
8. Velaphi SC, Westercamp M, Moleleki M, Pondo T, Dangor Z, Wolter N, von Gottberg A, Shang N, Demirjian A, Winchell JM, Diaz MH, Nakwa F, Okudo G, Wadula J, Cutland C, Schrag SJ, Madhi SA, Surveillance for incidence and etiology of early-onset neonatal sepsis in Soweto, South Africa. PLOS ONE 14, e0214077 (2019). [PubMed: 30970036]
9. Saha SK, Schrag SJ, El Arifeen S, Mullany LC, Shahidul Islam M, Shang N, Qazi SA, Zaidi AKM, Bhutta ZA, Bose A, Panigrahi P, Soofi SB, Connor NE, Mitra DK, Isaac R, Winchell JM, Arvay ML, Islam M, Shafiq Y, Nisar I, Baloch B, Kabir F, Ali M, Diaz MH, Satpathy R, Nanda P, Padhi BK, Parida S, Hotwani A, Hasanuzzaman M, Ahmed S, Belal Hossain M, Ariff S, Ahmed I, Ibne Moin SM, Mahmud A, Waller JL, Rafiqullah I, Quaiyum MA, Begum N, Balaji V, Halen J, Nawshad Uddin Ahmed ASM, Weber MW, Hamer DH, Hibberd PL, Sadeq-Ur Rahman Q, Mogan VR, Hossain T, McGee L, Anandan S, Liu A, Panigrahi K, Abraham AM, Baqui AH, Causes and incidence of community-acquired serious infections among young children in south Asia (ANISA): An observational cohort study. Lancet 392, 145–159 (2018). [PubMed: 30025808]
10. Biering-Sørensen S, Aaby P, Lund N, Monteiro I, Jensen KJ, Eriksen HB, Schaltz-Buchholzer F, Jorgensen ASP, Rodrigues A, Fisker AB, Benn CS, Early BCG-Denmark and neonatal mortality among infants weighing <2500 g: A randomized controlled trial. Clin. Infect. Dis 65, 1183–1190 (2017). [PubMed: 29579158]
11. Aaby P, Roth A, Ravn H, Napirna BM, Rodrigues A, Lisse IM, Stensballe L, Diness BR, Lausch KR, Lund N, Biering-Sorensen S, Whittle H, Benn CS, Randomized trial of BCG vaccination at birth to low-birth-weight children: Beneficial nonspecific effects in the neonatal period? J. Infect. Dis 204, 245–252 (2011). [PubMed: 21673035]
12. de Bree LCJ, Koeken V, Joosten LAB, Aaby P, Benn CS, van Crevel R, Netea MG, Non-specific effects of vaccines: Current evidence and potential implications. Semin. Immunol 39, 35–43 (2018). [PubMed: 30007489]

13. Goodridge HS, Ahmed SS, Curtis N, Kollmann TR, Levy O, Netea MG, Pollard AJ, van Crevel R, Wilson CB, Harnessing the beneficial heterologous effects of vaccination. Nat. Rev. Immunol 16, 392–400 (2016). [PubMed: 27157064]

14. WHO/SAGE, Meeting of the strategic advisory group of experts on immunization, April 2014 – Conclusions and recommendations. Wkly. Epidemiol. Rec 89, 233–236 (2014).

15. Higgins JPT, Soares-Weiser K, Reingold A, Systematic review of the non-specifi c eff ects of BCG, DTP and measles containing vaccines, WHO, Ed. (WHO, 2014), vol. 2015.

16. Blok BA, Arts RJ, van Crevel R, Benn CS, Netea MG, Trained innate immunity as underlying mechanism for the long-term, nonspecific effects of vaccines. J. Leukoc. Biol 98, 347–356 (2015). [PubMed: 26150551]

17. Freyne B, Marchant A, Curtis N, BCG-associated heterologous immunity, a historical perspective: Experimental models and immunological mechanisms. Trans. R. Soc. Trop. Med. Hyg 109, 46–51 (2015). [PubMed: 25573108]

18. Wynn JL, Scumpia PO, Delano MJ, O'Malley KA, Ungaro R, Abouhamze A, Moldawer LL, Increased mortality and altered immunity in neonatal sepsis produced by generalized peritonitis. Shock 28, 675–683 (2007). [PubMed: 17621256]

19. Wynn JL, Scumpia PO, Winfield RD, Delano MJ, Kelly-Scumpia K, Barker T, Ungaro R, Levy O, Moldawer LL, Defective innate immunity predisposes murine neonates to poor sepsis outcome but is reversed by TLR agonists. Blood 112, 1750–1758 (2008). [PubMed: 18591384]

20. Cuenca AG, Wynn JL, Kelly-Scumpia KM, Scumpia PO, Vila L, Delano MJ, Mathews E, Wallet SM, Reeves WH, Behrns KE, Nacionales DC, Efron PA, Kunkel SL, Moldawer LL, Critical role for CXC ligand 10/CXC receptor 3 signaling in the murine neonatal response to sepsis. Infect. Immun 79, 2746–2754 (2011). [PubMed: 21518789]

21. Cuenca AG, Joiner DN, Gentile LF, Cuenca AL, Wynn JL, Kelly-Scumpia KM, Scumpia PO, Behrns KE, Efron PA, Nacionales D, Lui C, Wallet SM, Reeves WH, Mathews CE, Moldawer LL, TRIF-dependent innate immune activation is critical for survival to neonatal gram-negative sepsis. J. Immunol 194, 1169–1177 (2015). [PubMed: 25548220]

22. Cuenca AG, Cuenca AL, Gentile LF, Efron PA, Islam S, Moldawer LL, Kays DW, Larson SD, Delayed emergency myelopoiesis following polymicrobial sepsis in neonates. Innate Immun. 21, 386–391 (2015). [PubMed: 25106654]

23. Gentile LF, Cuenca AL, Cuenca AG, Nacionales DC, Ungaro R, Efron PA, Moldawer LL, Larson SD, Improved emergency myelopoiesis and survival in neonatal sepsis by caspase-1/11 ablation. Immunology 145, 300–311 (2015). [PubMed: 25684123]

24. Brook B, Harbeson D, Ben-Othman R, Viemann D, Kollmann TR, Newborn susceptibility to infection vs. disease depends on complex in vivo interactions of host and pathogen. Semin. Immunopathol 39, 615–625 (2017). [PubMed: 29098373]

25. Kollmann TR, Kampmann B, Mazmanian SK, Marchant A, Levy O, Protecting the newborn and young infant from infectious diseases: Lessons from immune ontogeny. Immunity 46, 350–363 (2017). [PubMed: 28329702]

26. Nauseef WM, Borregaard N, Neutrophils at work. Nat. Immunol 15, 602–611 (2014). [PubMed: 24940954]

27. Pena OM, Hancock DG, Lyle NH, Linder A, Russell JA, Xia J, Fjell CD, Boyd JH, Hancock RE, An endotoxin tolerance signature predicts sepsis and organ dysfunction at initial clinical presentation. EBioMedicine 1, 64–71 (2014). [PubMed: 25685830]

28. O'Brien XM, Biron BM, Reichner JS, Consequences of extracellular trap formation in sepsis. Curr. Opin. Hematol 24, 66–71 (2017). [PubMed: 27820735]

29. Brook B, Amenyogbe N, Ben-Othman R, Cai B, Harbeson D, Francis F, Liu AC, Varankovich N, Wynn J, Kollmann TR, A controlled mouse model for neonatal polymicrobial sepsis. J. Vis. Exp 10.3791/58574, (2019).

30. Manz MG, Boettcher S, Emergency granulopoiesis. Nat. Rev. Immunol 14, 302–314 (2014). [PubMed: 24751955]

31. Boettcher S, Manz MG, Sensing and translation of pathogen signals into demand-adapted myelopoiesis. Curr. Opin. Hematol 23, 5–10 (2016). [PubMed: 26554891]

32. Yadav M, Schorey JS, The beta-glucan receptor dectin-1 functions together with TLR2 to mediate macrophage activation by mycobacteria. Blood 108, 3168–3175 (2006). [PubMed: 16825490]
33. Kleinnijenhuis J, Quintin J, Preijers F, Joosten LA, Ifrim DC, Saeed S, Jacobs C, van Loenhout J, de Jong D, Stunnenberg HG, Xavier RJ, van der Meer JW, van Crevel R, Netea MG, Bacille Calmette-Guerin induces NOD2-dependent nonspecific protection from reinfection via epigenetic reprogramming of monocytes. Proc. Natl. Acad. Sci. U.S.A 109, 17537–17542 (2012). [PubMed: 22988082]
34. Lee AH, Shannon CP, Amenyogbe N, Bennike TB, Diray-Arce J, Idoko O, Gill EE, Ben-Othman R, Pomat WS, van Haren S, Lê Cao KA, Cox M, Darboe A, Falsafi R, Ferrari D, Harbeson DJ, He D, Bing C, Hinshaw SJ, Ndure J, Njie-Jobe J, Pettengill MA, Richmond PC, Ford R, Saleu G, Masiria G, Kirarock MJPW, Roberts E, Malek M, Sanchez-Schmitz G, Singh A, Angelidou A, Smolen KK, Brinkman RR, Ozonoff A, Hancock REW, van den Biggelaar A, Steen H, Tebbutt SJ, Kampmann B, Levy O, Kollmann TR, Dynamic molecular changes during the first week of human life follow a robust developmental trajectory. Nat. Commun 10, 1092 (2019). [PubMed: 30862783]
35. Maheshwari A, Neutropenia in the newborn. Curr. Opin. Hematol 21, 43–49 (2014). [PubMed: 24322487]
36. Walk J, de Bree LCJ, Graumans W, Stoter R, van Gemert GJ, van de Vegte-Bolmer M, Teelen K, Hermsen CC, Arts RJW, Behet MC, Keramati F, Moorlag S, Yang ASP, van Crevel R, Aaby P, de Mast Q, van der Ven A, Stabell Benn C, Netea MG, Sauerwein RW, Outcomes of controlled human malaria infection after BCG vaccination. Nat. Commun 10, 874 (2019). [PubMed: 30787276]
37. Arts RJW, Moorlag S, Novakovic B, Li Y, Wang SY, Oosting M, Kumar V, Xavier RJ, Wijmenga C, Joosten LAB, Reusken C, Benn CS, Aaby P, Koopmans MP, Stunnenberg HG, van Crevel R, Netea MG, BCG vaccination protects against experimental viral infection in humans through the induction of cytokines associated with trained immunity. Cell Host Microbe 23, 89–100.e5 (2018). [PubMed: 29324233]
38. Angelidou A, Conti MG, Diray-Arce J, Benn CS, Shann F, Netea MG, Liu M, Potluri LP, Sanchez-Schmitz G, Husson R, Ozonoff A, Kampmann B, van Haren SD, Levy O, Licensed Bacille Calmette-Guérin (BCG) formulations differ markedly in bacterial viability, RNA content and innate immune activation. Vaccine 38, 2229–2240 (2020). [PubMed: 32005538]
39. Carr R, Modi N, Doré C, G-CSF and GM-CSF for treating or preventing neonatal infections. Cochrane Database Syst. Rev 2003, CD003066 (2003).
40. Liu MH, Lin AH, Lee HF, Ko HK, Lee TS, Kou YR, Paeonol attenuates cigarette smoke-induced lung inflammation by inhibiting ROS-sensitive inflammatory signaling. Mediators Inflamm. 2014, 651890 (2014). [PubMed: 25165413]
41. Yang J, Qi F, Gu H, Zou J, Yang Y, Yuan Q, Yao Z, Neonatal BCG vaccination of mice improves neurogenesis and behavior in early life. Brain Res. Bull 120, 25–33 (2016). [PubMed: 26536170]
42. Brynjolfsson SF, Bjarnarson SP, Mori E, Del Giudice G, Jonsdottir I, Concomitant administration of Mycobacterium bovis BCG with the meningococcal C conjugate vaccine to neonatal mice enhances antibody response and protective efficacy. Clin. Vaccine Immunol 18, 1936–1942 (2011). [PubMed: 21900528]
43. Saubi N, Im EJ, Fernandez-Lloris R, Gil O, Cardona PJ, Gatell JM, Hanke T, Joseph J, Newborn mice vaccination with BCG.HIVA$^{222}$ + MVA.HIVA enhances HIV-1-specific immune responses: Influence of age and immunization routes. Clin. Dev. Immunol 2011, 516219 (2011). [PubMed: 21603216]
44. Pryde JG, Walker A, Rossi AG, Hannah S, Haslett C, Temperature-dependent arrest of neutrophil apoptosis. Failure of Bax insertion into mitochondria at 15 degrees C prevents the release of cytochrome c. J. Biol. Chem 275, 33574–33584 (2000). [PubMed: 10896657]
45. Deniset JF, Surewaard BG, Lee WY, Kubes P, Splenic Ly6G$^{high}$ mature and Ly6G$^{int}$ immature neutrophils contribute to eradication of S. *pneumoniae*. J. Exp. Med 214, 1333–1350 (2017). [PubMed: 28424248]
46. Boehm M, Bukosza EN, Huttary N, Herzog R, Aufricht C, Kratochwill K, Gebeshuber CA, A systems pharmacology workflow with experimental validation to assess the potential of anakinra for treatment of focal and segmental glomerulosclerosis. PLOS ONE 14, e0214332 (2019). [PubMed: 30921378]

47. Aden U, Favrais G, Plaisant F, Winerdal M, Felderhoff-Mueser U, Lampa J, Lelièvre V, Gressens P, Systemic inflammation sensitizes the neonatal brain to excitotoxicity through a pro-/anti-inflammatory imbalance: Key role of TNFα pathway and protection by etanercept. Brain Behav. Immun 24, 747–758 (2010). [PubMed: 19861157]
48. Pasquier J, Gosset M, Geyl C, Hoarau-Vechot J, Chevrot A, Pocard M, Mirshahi M, Lis R, Rafii A, Touboul C, CCL2/CCL5 secreted by the stroma induce IL-6/PYK2 dependent chemoresistance in ovarian cancer. Mol. Cancer 17, 47 (2018). [PubMed: 29455640]
49. Gardner JC, Noel JG, Nikolaidis NM, Karns R, Aronow BJ, Ogle CK, F. X. McCormack, G-CSF drives a posttraumatic immune program that protects the host from infection. J. Immunol 192, 2405–2417 (2014). [PubMed: 24470495]
50. Buechler MB, Teal TH, Elkon KB, Hamerman JA, Cutting edge: Type I IFN drives emergency myelopoiesis and peripheral myeloid expansion during chronic TLR7 signaling. J. Immunol 190, 886–891 (2013). [PubMed: 23303674]
51. Leek JT, Johnson WE, Parker HS, Jaffe AE, Storey JD, The sva package for removing batch effects and other unwanted variation in high-throughput experiments. Bioinformatics 28, 882–883 (2012). [PubMed: 22257669]
52. Lê Cao KA, Boitard S, Besse P, Sparse PLS discriminant analysis: Biologically relevant feature selection and graphical displays for multiclass problems. BMC Bioinformatics 12, 253 (2011). [PubMed: 21693065]
53. Benita Y, Cao Z, Giallourakis C, Li C, Gardet A, Xavier RJ, Gene enrichment profiles reveal T-cell development, differentiation, and lineage-specific transcription factors including ZBTB25 as a novel NF-AT repressor. Blood 115, 5376–5384 (2010). [PubMed: 20410506]
54. Subramanian A, Tamayo P, Mootha VK, Mukherjee S, Ebert BL, Gillette MA, Paulovich A, Pomeroy SL, Golub TR, Lander ES, Mesirov JP, Gene set enrichment analysis: A knowledge-based approach for interpreting genome-wide expression profiles. Proc. Natl. Acad. Sci. U.S.A 102, 15545–15550 (2005). [PubMed: 16199517]
55. Fu X, Lyu X, Liu H, Zhong D, Xu Z, He F, Huang G, Chlorogenic acid inhibits BAFF expression in collagen-induced arthritis and human synoviocyte MH7A cells by modulating the activation of the NF-κB signaling pathway. J. Immunol. Res 2019, 8042097 (2019). [PubMed: 31240234]
56. Badr G, Borhis G, Lefevre EA, Chaoul N, Deshayes F, Dessirier V, Lapree G, Tsapis A, Richard Y, BAFF enhances chemotaxis of primary human B cells: A particular synergy between BAFF and CXCL13 on memory B cells. Blood 111, 2744–2754 (2008). [PubMed: 18172003]
57. Walters S, Webster KE, Sutherland A, Gardam S, Groom J, Liuwantara D, Marino E, Thaxton J, Weinberg A, Mackay F, Brink R, Sprent J, Grey ST, Increased CD4+Foxp3+ T cells in BAFF-transgenic mice suppress T cell effector responses. J. Immunol 182, 793–801 (2009). [PubMed: 19124722]
58. Schneider MR, Dahlhoff M, Herbach N, Renner-Mueller I, Dalke C, Puk O, Graw J, Wanke R, Wolf E, Betacellulin overexpression in transgenic mice causes disproportionate growth, pulmonary hemorrhage syndrome, and complex eye pathology. Endocrinology 146, 5237–5246 (2005). [PubMed: 16179416]
59. Laudanski P, Lemancewicz A, Kuc P, Charkiewicz K, Ramotowska B, Kretowska M, Jasinska E, Raba G, Karwasik-Kajszczarek K, Kraczkowski J, Laudanski T, Chemokines profiling of patients with preterm birth. Mediators Inflamm. 2014, 185758 (2014). [PubMed: 24876667]
60. Mostafa GA, Al-Ayadhi LY, The possible link between elevated serum levels of epithelial cell-derived neutrophil-activating peptide-78 (ENA-78/CXCL5) and autoimmunity in autistic children. Behav. Brain Funct 11, 11 (2015). [PubMed: 25871636]
61. Mancuso RI, Miyaji EN, Silva CCF, Portaro FV, Soares-Schanoski A, Ribeiro OG, Oliveira MLS, Impaired expression of CXCL5 and matrix metalloproteinases in the lungs of mice with high susceptibility to Streptococcus pneumoniae infection. Immun. Inflamm. Dis 6, 128–142 (2017). [PubMed: 29119707]
62. Osuchowski MF, Welch K, Siddiqui J, Remick DG, Circulating cytokine/inhibitor profiles reshape the understanding of the SIRS/CARS continuum in sepsis and predict mortality. J. Immunol 177, 1967–1974 (2006). [PubMed: 16849510]

63. Bhatty M, Jan BL, Tan W, Pruett SB, Nanduri B, Role of acute ethanol exposure and TLR4 in early events of sepsis in a mouse model. Alcohol 45, 795–803 (2011). [PubMed: 21872420]
64. Shrum B, Anantha RV, Xu SX, Donnelly M, Haeryfar SM, McCormick JK, Mele T, A robust scoring system to evaluate sepsis severity in an animal model. BMC. Res. Notes 7, 233 (2014). [PubMed: 24725742]
65. Souza-Fonseca-Guimaraes F, Parlato M, Fitting C, Cavaillon JM, Adib-Conquy M, NK cell tolerance to TLR agonists mediated by regulatory T cells after polymicrobial sepsis. J. Immunol 188, 5850–5858 (2012). [PubMed: 22566566]
66. Mera S, Tatulescu D, Cismaru C, Bondor C, Slavcovici A, Zanc V, Carstina D, Oltean M, Multiplex cytokine profiling in patients with sepsis. Apmis 119, 155–163 (2011). [PubMed: 21208283]
67. Mathias B, Szpila BE, Moore FA, Efron PA, Moldawer LL, A review of GM-CSF therapy in sepsis. Medicine 94, e2044 (2015). [PubMed: 26683913]
68. Wolach B, Gavrieli R, Pomeranz A, Effect of granulocyte and granulocyte macrophage colony stimulating factors (G-CSF and GM-CSF) on neonatal neutrophil functions. Pediatr. Res 48, 369–373 (2000). [PubMed: 10960505]
69. Brown KA, Brain SD, Pearson JD, Edgeworth JD, Lewis SM, Treacher DF, Neutrophils in development of multiple organ failure in sepsis. Lancet 368, 157–169 (2006). [PubMed: 16829300]
70. Jin L, Batra S, Jeyaseelan S, Diminished neutrophil extracellular trap (NET) formation is a novel innate immune deficiency induced by acute ethanol exposure in polymicrobial sepsis, which can be rescued by CXCL1. PLOS Pathog. 13, e1006637 (2017). [PubMed: 28922428]
71. Luo CJ, Luo F, Zhang L, Xu Y, Cai GY, Fu B, Feng Z, Sun XF, Chen XM, Knockout of interleukin-17A protects against sepsis-associated acute kidney injury. Ann. Intensive Care 6, 56 (2016). [PubMed: 27334720]
72. Tilg H, Peschel C, Interferon-alpha and its effects on the cytokine cascade: A pro- and anti-inflammatory cytokine. Leuk. Lymphoma 23, 55–60 (1996). [PubMed: 9021686]
73. Paludan SR, Synergistic action of pro-inflammatory agents: Cellular and molecular aspects. J. Leukoc. Biol 67, 18–25 (2000). [PubMed: 10647993]
74. Kox WJ, Volk T, Kox SN, Volk HD, Immunomodulatory therapies in sepsis. Intensive Care Med. 26 (suppl. 1), S124–S128 (2000). [PubMed: 10786969]
75. Gao F, Yang YZ, Feng XY, Fan TT, Jiang L, Guo R, Liu Q, Interleukin-27 is elevated in sepsis-induced myocardial dysfunction and mediates inflammation. Cytokine 88, 1–11 (2016). [PubMed: 27525353]
76. Kong W, Yen JH, Vassiliou E, Adhikary S, Toscano MG, Ganea D, Docosahexaenoic acid prevents dendritic cell maturation and in vitro and in vivo expression of the IL-12 cytokine family. Lipids Health Dis. 9, 12 (2010). [PubMed: 20122166]
77. Teoh H, Quan A, Bang KW, Wang G, Lovren F, Vu V, Haitsma JJ, Szmitko PE, Al-Omran M, Wang CH, Gupta M, Peterson MD, Zhang H, Chan L, Freedman J, Sweeney G, Verma S, Adiponectin deficiency promotes endothelial activation and profoundly exacerbates sepsis-related mortality. Am. J. Physiol. Endocrinol. Metab 295, E658–E664 (2008). [PubMed: 18628355]
78. Kalechman Y, Gafter U, Gal R, Rushkin G, Yan D, Albeck M, Sredni B, Anti-IL-10 therapeutic strategy using the immunomodulator AS101 in protecting mice from sepsis-induced death: Dependence on timing of immunomodulating intervention. J. Immunol 169, 384–392 (2002). [PubMed: 12077268]
79. Brito LF, Oliveira HBM, das Neves Selis N, E Souza CLS, Junior MNS, de Souza EP, Silva L, de Souza Nascimento F, Amorim AT, Campos GB, de Oliveira MV, Yatsuda R, Timenetsky J, Marques LM, Anti-inflammatory activity of β-caryophyllene combined with docosahexaenoic acid in a model of sepsis induced by Staphylococcus aureus in mice. J. Sci. Food Agric 99, 5870–5880 (2019). [PubMed: 31206687]
80. Sugitharini V, Prema A, Berla Thangam E, Inflammatory mediators of systemic inflammation in neonatal sepsis. Inflamm. Res 62, 1025–1034 (2013). [PubMed: 24013483]

81. Guo Y, Luan L, Patil NK, Wang J, Bohannon JK, Rabacal W, Fensterheim BA, Hernandez A, Sherwood ER, IL-15 enables septic shock by maintaining NK cell integrity and function. J. Immunol 198, 1320–1333 (2017). [PubMed: 28031340]
82. Ghosh S, DeCoffe D, Brown K, Rajendiran E, Estaki M, Dai C, Yip A, Gibson DL, Fish oil attenuates omega-6 polyunsaturated fatty acid-induced dysbiosis and infectious colitis but impairs LPS dephosphorylation activity causing sepsis. PLOS ONE 8, e55468 (2013). [PubMed: 23405155]
83. Flierl MA, Rittirsch D, Gao H, Hoesel LM, Nadeau BA, Day DE, Zetoune FS, Sarma JV, Huber-Lang MS, Ferrara JL, Ward PA, Adverse functions of IL-17A in experimental sepsis. FASEB J. 22, 2198–2205 (2008). [PubMed: 18299333]
84. Joshi A, Pancari G, Cope L, Bowman EP, Cua D, Proctor RA, McNeely T, Immunization with Staphylococcus aureus iron regulated surface determinant B (IsdB) confers protection via Th17/IL17 pathway in a murine sepsis model. Hum. Vaccin. Immunother 8, 336–346 (2012). [PubMed: 22327491]
85. Wozniak KL, Hardison SE, Kolls JK, Wormley FL, Role of IL-17A on resolution of pulmonary *C. neoformans* infection. PLOS ONE 6, e17204 (2011). [PubMed: 21359196]
86. Wang YC, Liu QX, Zheng Q, Liu T, Xu XE, Liu XH, Gao W, Bai XJ, Li ZF, Dihydromyricetin alleviates sepsis-induced acute lung injury through inhibiting NLRP3 inflammasome-dependent pyroptosis in mice model. Inflammation 42, 1301–1310 (2019). [PubMed: 30887396]
87. Burmeister AR, Johnson MB, Yaemmongkol JJ, Marriott I, Murine astrocytes produce IL-24 and are susceptible to the immunosuppressive effects of this cytokine. J. Neuroinflammation 16, 55 (2019). [PubMed: 30825881]
88. Benjamin JT, Moore DJ, Bennett C, van der Meer R, Royce A, Loveland R, Wynn JL, Cutting edge: IL-1α and not IL-1β drives IL-1R1-dependent neonatal murine sepsis lethality. J. Immunol 201, 2873–2878 (2018). [PubMed: 30305325]
89. Lawrence SM, Corriden R, Nizet V, The ontogeny of a neutrophil: Mechanisms of granulopoiesis and homeostasis. Microbiol. Mol. Biol. Rev 82, e00057–17 (2018). [PubMed: 29436479]
90. Cao C, Chai Y, Shou S, Wang J, Huang Y, Ma T, Toll-like receptor 4 deficiency increases resistance in sepsis-induced immune dysfunction. Int. Immunopharmacol 54, 169–176 (2018). [PubMed: 29149705]
91. Weber GF, Schlautkotter S, Kaiser-Moore S, Altmayr F, Holzmann B, Weighardt H, Inhibition of interleukin-22 attenuates bacterial load and organ failure during acute polymicrobial sepsis. Infect. Immun 75, 1690–1697 (2007). [PubMed: 17261606]
92. Aggarwal S, Gurney AL, IL-17: Prototype member of an emerging cytokine family. J. Leukoc. Biol 71, 1–8 (2002). [PubMed: 11781375]
93. Cao J, Xu F, Lin S, Song Z, Zhang L, Luo P, Xu H, Li D, Zheng K, Ren G, Yin Y, IL-27 controls sepsis-induced impairment of lung antibacterial host defence. Thorax 69, 926–937 (2014). [PubMed: 25074706]
94. Zhang D, McQuestin OJ, Mellefont LA, Ross T, The influence of non-lethal temperature on the rate of inactivation of vegetative bacteria in inimical environments may be independent of bacterial species. Food Microbiol. 27, 453–459 (2010). [PubMed: 20417393]
95. Borriello F, Galdiero MR, Varricchi G, Loffredo S, Spadaro G, Marone G, Innate immune modulation by GM-CSF and IL-3 in health and disease. Int. J. Mol. Sci 20, E834 (2019). [PubMed: 30769926]
96. Weber GF, Chousterman BG, He S, Fenn AM, Nairz M, Anzai A, Brenner T, Uhle F, Iwamoto Y, Robbins CS, Noiret L, Maier SL, Zonnchen T, Rahbari NN, Scholch S, Klotzsche-von Ameln A, Chavakis T, Weitz J, Hofer S, Weigand MA, Nahrendorf M, Weissleder R, Swirski FK, Interleukin-3 amplifies acute inflammation and is a potential therapeutic target in sepsis. Science 347, 1260–1265 (2015). [PubMed: 25766237]
97. Cho BS, Kim JO, Ha DH, Yi YW, Exosomes derived from human adipose tissue-derived mesenchymal stem cells alleviate atopic dermatitis. Stem Cell Res. Ther 9, 187 (2018). [PubMed: 29996938]

98. Gu X, Wei C, Zhu X, Lu F, Sheng B, Zang X, Effect of interleukin-31 on septic shock through regulating inflammasomes and interleukin-1 β. Exp. Ther. Med 16, 171–177 (2018). [PubMed: 29896237]
99. Staurengo-Ferrari L, Ruiz-Miyazawa KW, Pinho-Ribeiro FA, Domiciano TP, Fattori V, Mizokami SS, Pelayo JS, Bordignon J, Figueiredo F, Casagrande R, Miranda KM, Verri WA Jr., The nitroxyl donor Angeli's salt ameliorates *Staphylococcus aureus*-induced septic arthritis in mice. Free Radic. Biol. Med 108, 487–499 (2017). [PubMed: 28419865]
100. Alves-Filho JC, Sonego F, Souto FO, Freitas A, Verri WA Jr., Auxiliadora-Martins M, Basile-Filho A, McKenzie AN, Xu D, Cunha FQ, Liew FY, Interleukin-33 attenuates sepsis by enhancing neutrophil influx to the site of infection. Nat. Med 16, 708–712 (2010). [PubMed: 20473304]
101. Mitchell PD, Salter BM, Oliveria JP, El-Gammal A, Tworek D, Smith SG, Sehmi R, Gauvreau GM, O Apos Byrne PM, IL-33 and its receptor ST2 after inhaled allergen challenge in allergic asthmatics. Int. Arch. Allergy Immunol 176, 133–142 (2018). [PubMed: 29694974]
102. Yang Q, Luo J, Lv H, Wen T, Shi B, Liu X, Zeng N, Pulegone inhibits inflammation via suppression of NLRP3 inflammasome and reducing cytokine production in mice. Immunopharmacol. Immunotoxicol 41, 420–427 (2019). [PubMed: 31134844]
103. Xu H, Xu J, Xu L, Jin S, Turnquist HR, Hoffman R, Loughran P, Billiar TR, Deng M, Interleukin-33 contributes to ILC2 activation and early inflammation-associated lung injury during abdominal sepsis. Immunol. Cell Biol 96, 935–947 (2018). [PubMed: 29672927]
104. Pedersen I, David M, MicroRNAs in the immune response. Cytokine 43, 391–394 (2008). [PubMed: 18701320]
105. Opal SM, Keith JC, Palardy JE, Parejo N, Recombinant human interleukin-11 has anti-inflammatory actions yet does not exacerbate systemic Listeria infection. J. Infect. Dis 181, 754–756 (2000). [PubMed: 10669370]
106. Unsinger J, McGlynn M, Kasten KR, Hoekzema AS, Watanabe E, Muenzer JT, McDonough JS, Tschoep J, Ferguson TA, McDunn JE, Morre M, Hildeman DA, Caldwell CC, Hotchkiss RS, IL-7 promotes T cell viability, trafficking, and functionality and improves survival in sepsis. J. Immunol 184, 3768–3779 (2010). [PubMed: 20200277]
107. Goswami R, Kaplan MH, A brief history of IL-9. J. Immunol 186, 3283–3288 (2011). [PubMed: 21368237]
108. Grohmann U, Van Snick J, Campanile F, Silla S, Giampietri A, Vacca C, Renauld JC, Fioretti MC, Puccetti P, IL-9 protects mice from Gram-negative bacterial shock: Suppression of TNF-α, IL-12, and IFN-γ, and induction of IL-10. J. Immunol 164, 4197–4203 (2000). [PubMed: 10754315]
109. Lang S, Li L, Wang X, Sun J, Xue X, Xiao Y, Zhang M, Ao T, Wang J, CXCL10/IP-10 neutralization can ameliorate lipopolysaccharide-induced acute respiratory distress syndrome in rats. PLOS ONE 12, e0169100 (2017). [PubMed: 28046003]
110. Kelly-Scumpia KM, Scumpia PO, Delano MJ, Weinstein JS, Cuenca AG, Wynn JL, Moldawer LL, Type I interferon signaling in hematopoietic cells is required for survival in mouse polymicrobial sepsis by regulating CXCL10. J. Exp. Med 207, 319–326 (2010). [PubMed: 20071504]
111. Sharma A, Steven S, Bosmann M, The pituitary gland prevents shock-associated death by controlling multiple inflammatory mediators. Biochem. Biophys. Res. Commun 509, 188–193 (2019). [PubMed: 30579593]
112. Lin J, Yan GT, Xue H, Hao XH, Zhang K, Wang LH, Leptin protects vital organ functions after sepsis through recovering tissue myeloperoxidase activity: An anti-inflammatory role resonating with indomethacin. Peptides 28, 1553–1560 (2007). [PubMed: 17681405]
113. Iskander KN, Vaickus M, Duffy ER, Remick DG, Shorter duration of post-operative antibiotics for cecal ligation and puncture does not increase inflammation or mortality. PLOS ONE 11, e0163005 (2016). [PubMed: 27669150]
114. Ramnath RD, Ng SW, Guglielmotti A, Bhatia M, Role of MCP-1 in endotoxemia and sepsis. Int. Immunopharmacol 8, 810–818 (2008). [PubMed: 18442784]

115. Matsumoto H, Ogura H, Shimizu K, Ikeda M, Hirose T, Matsuura H, Kang S, Takahashi K, Tanaka T, Shimazu T, The clinical importance of a cytokine network in the acute phase of sepsis. Sci. Rep 8, 13995 (2018). [PubMed: 30228372]

116. Wang Y, Wang F, Yang D, Tang X, Li H, Lv X, Lu D, Wang H, Berberine in combination with yohimbine attenuates sepsis-induced neutrophil tissue infiltration and multiorgan dysfunction partly via IL-10-mediated inhibition of CCR2 expression in neutrophils. Int. Immunopharmacol 35, 217–225 (2016). [PubMed: 27082997]

117. Marpegan L, Leone MJ, Katz ME, Sobrero PM, Bekinstein TA, Golombek DA, Diurnal variation in endotoxin-induced mortality in mice: Correlation with proinflammatory factors. Chronobiol. Int 26, 1430–1442 (2009). [PubMed: 19916840]

118. Demoule A, Divangahi M, Yahiaoui L, Danialou G, Gvozdic D, Petrof BJ, Chemokine receptor and ligand upregulation in the diaphragm during endotoxemia and Pseudomonas lung infection. Mediators Inflamm. 2009, 860565 (2009). [PubMed: 19421418]

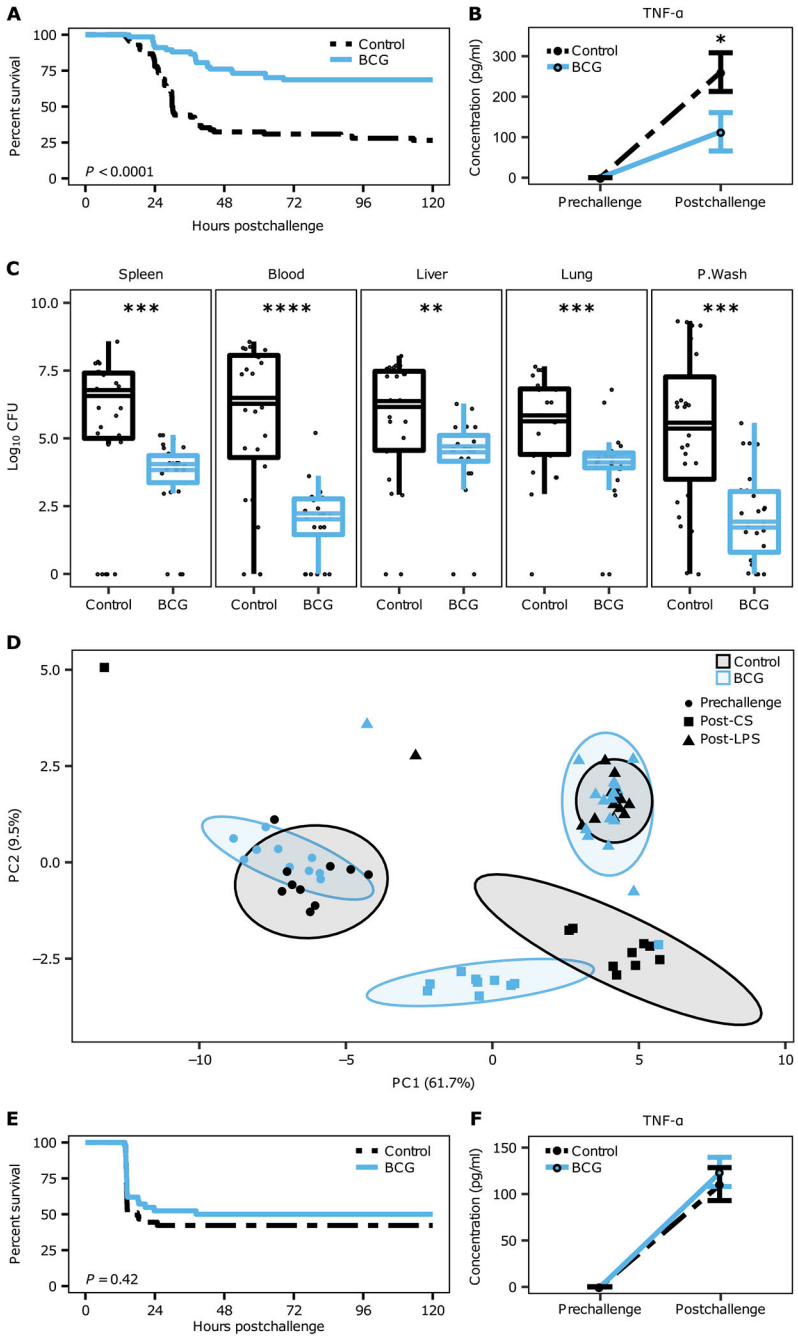


**Fig. 1. BCG protected neonatal mice from infectious, but not sterile septic death.**

(**A**) BCG-vaccinated mice demonstrated a significant increase in survival from neonatal polymicrobial sepsis (solid blue line) compared with controls (dashed black line) ($n$=67 per group, $P < 0.0001$). (**B**) BCG reduced tumor necrosis factor-α (TNF-α) production 24 hours after septic challenge, just before the maximal mortality period in this model ($n = 10$). (**C**) BCG vaccination reduced bacterial load across blood, organs, and peritoneal wash (P.Wash) ($n = 26$ to 27) 24 hours after sepsis. (**D**) Principal components analysis (PCA) of all cytokines prechallenge (circles, 3 days after vaccination), post–CS-induced sepsis (post-CS,

squares), and post-LPS challenge (post-LPS, triangles), colored by vaccination status (BCG, blue; control, black; $n = 10$ to 16 per group; individual cytokines in fig. S2 and summarized roles in table S1). (**E**) BCG did not protect mice from endotoxin shock ($n = 42$ to 45, $P = 0.42$). (**F**) BCG did not reduce TNF-α production 12 hours after LPS challenge, just before the maximal mortality period in this model ($n = 14$ to 16, $P = 0.96$). Statistical analysis by log-rank test (A and D); unpaired two-sided *t* test, Benjamini-Hochberg (BH) adjusted (B and E); and Wilcoxon rank-sum test BH adjusted (C). *$P < 0.05$, **$P < 0.01$, ***$P < 0.001$, and ****$P < 0.0001$.

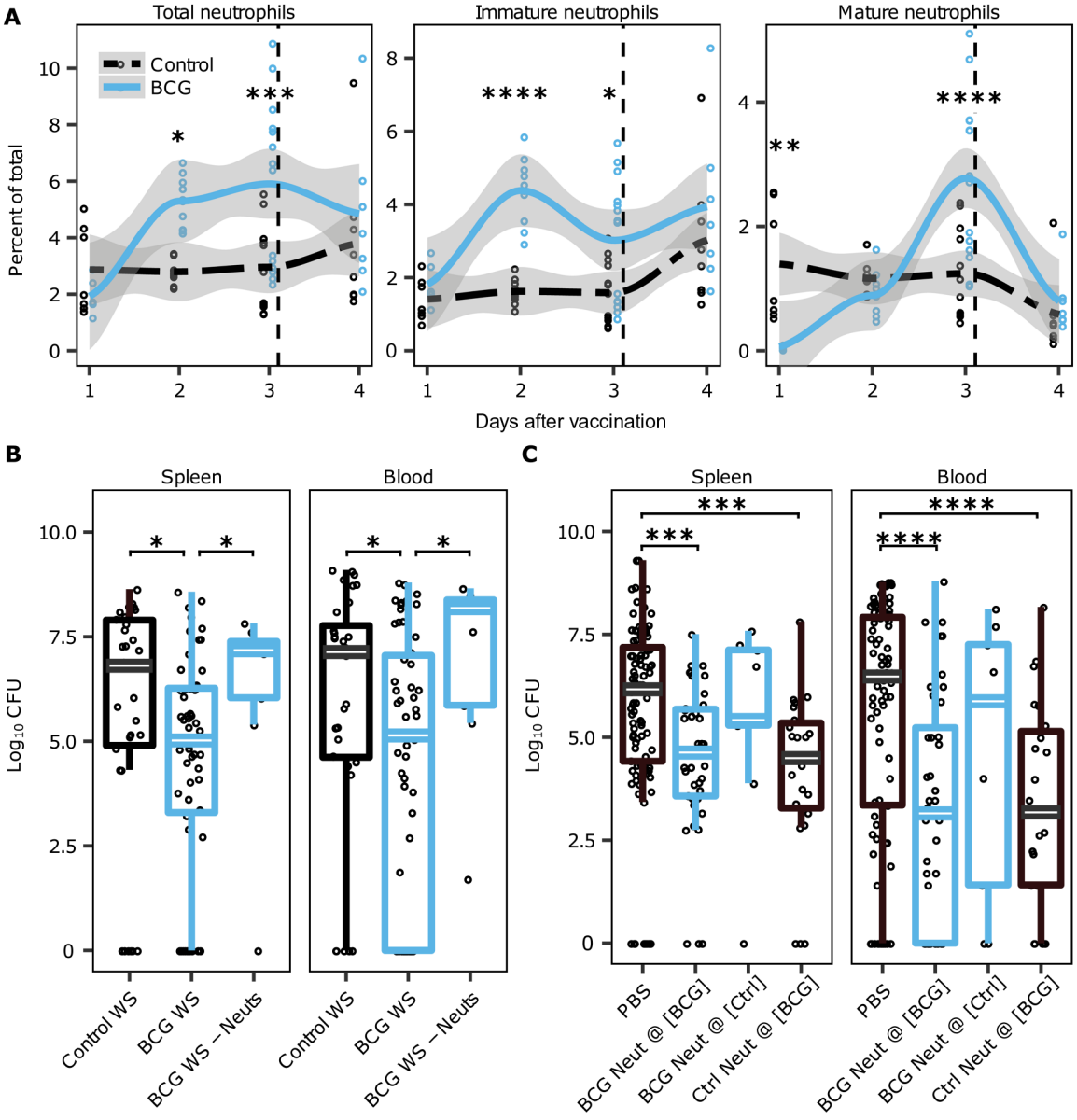


**Fig. 2. BCG-induced increase in neutrophil numbers was necessary and sufficient for protection.**

(**A**) BCG increased total neutrophils in the spleen, with immature and mature neutrophils peaking on days 2 and 3, respectively, after vaccination (BCG, solid blue line; control, dashed black line). Mature neutrophils mobilized from the spleen within 24 hours of CS challenge (vertical dotted line) ($n$ = 6 to 7, 10, 13 to 14, and 7 to 8 on days 1, 2, 3, and 4, respectively, with 95% CI presented in gray). (**B**) Adoptive transfer of splenocytes from BCG-vaccinated donors ("BCG WS") versus control splenocytes ("Control WS") reduced bacterial burden ($n$ = 55 and 32), but not if mature neutrophils were depleted from BCG-vaccinated spleens before adoptive transfer ("BCG WS – Neuts"; $n$ = 9). (**C**) Mature neutrophils purified from BCG-vaccinated donors and transferred at expected BCG-vaccinated numbers ("BCG Neut @ [BCG]"; $n$ = 40) reduced bacterial burden, whereas transfer of fewer cells, specifically the expected cell numbers in a control mouse ("BCG

Neut @ [Ctrl]"; $n = 9$), impaired bacterial clearance. Control donor neutrophils artificially increased to match BCG numbers ("Ctrl Neut @ [BCG]"; $n = 23$) were similarly protective as BCG-purified neutrophils (colored by donor mouse vaccination status; control, black; BCG, blue). Statistical analysis by BH-adjusted, unpaired two-sided *t* test (A) and Kruskal-Wallis rank-sum test unpaired Wilcoxon rank-sum test in (B) and (C) with $*P < 0.05$, $**P < 0.01$, $***P < 0.001$, and $****P < 0.0001$.

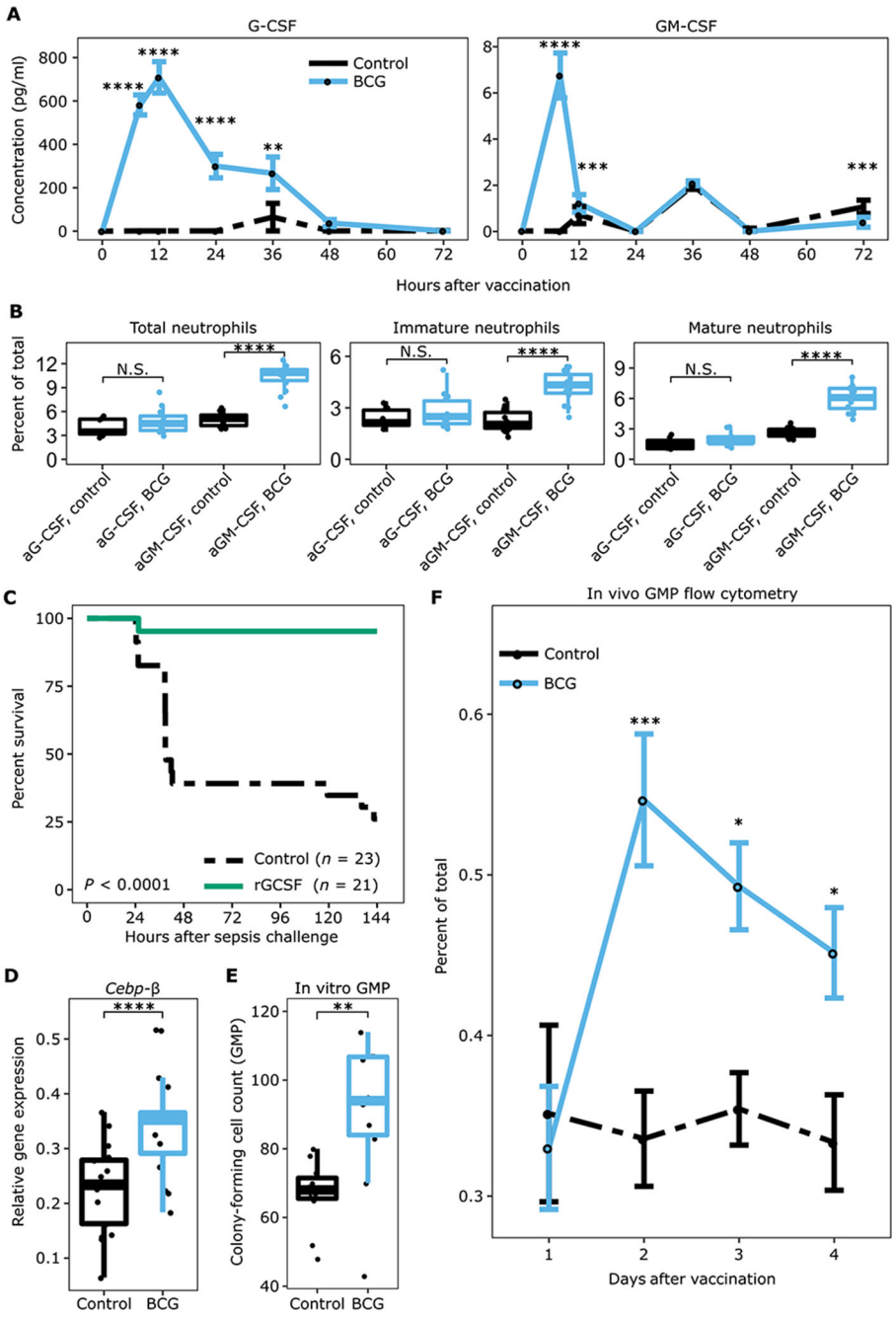


**Fig. 3. BCG vaccination–induced EG.**

(**A**) BCG (blue solid line) versus control (black dashed line) induced production of EG-supporting cytokines within 8 to 12 hours after vaccination ($n$ = 10 per group and time point). (**B**) Antibody-mediated blocking inhibited EG when targeting G-CSF, but not GM-CSF ($n$ = 8 to 14). N.S., not significant. (**C**) Recombinant G-CSF (rG-CSF) given at 0.1 μg rG-CSF/g mouse induced BCG-like protection against sepsis. (**D**) *Cebp*-β RNA expression increased in the spleens of BCG-vaccinated mice 12 hours after vaccination presented as relative gene expression compared with the 18*S* housekeeping gene (calculated by $2^{\Delta\Delta CT}$, $n$ = 17 per group). (**E**) GMP numbers increased in the spleens 2 days after vaccination, as

determined by in vitro culture ($n = 11$ per group). (**F**) Kinetics of BCG-induced splenocyte GMP increase after vaccination, identified by flow cytometry ($n = 6$ to 7 per group and time point; gating strategy in fig. S11). Statistical analysis by unpaired two-sided *t* test for (A), (B), and (D) to (F), with BH adjustment for (A) and (F), and log-rank test for (C). *$P < 0.05$, **$P < 0.01$, ***$P < 0.001$, and ****$P < 0.0001$.

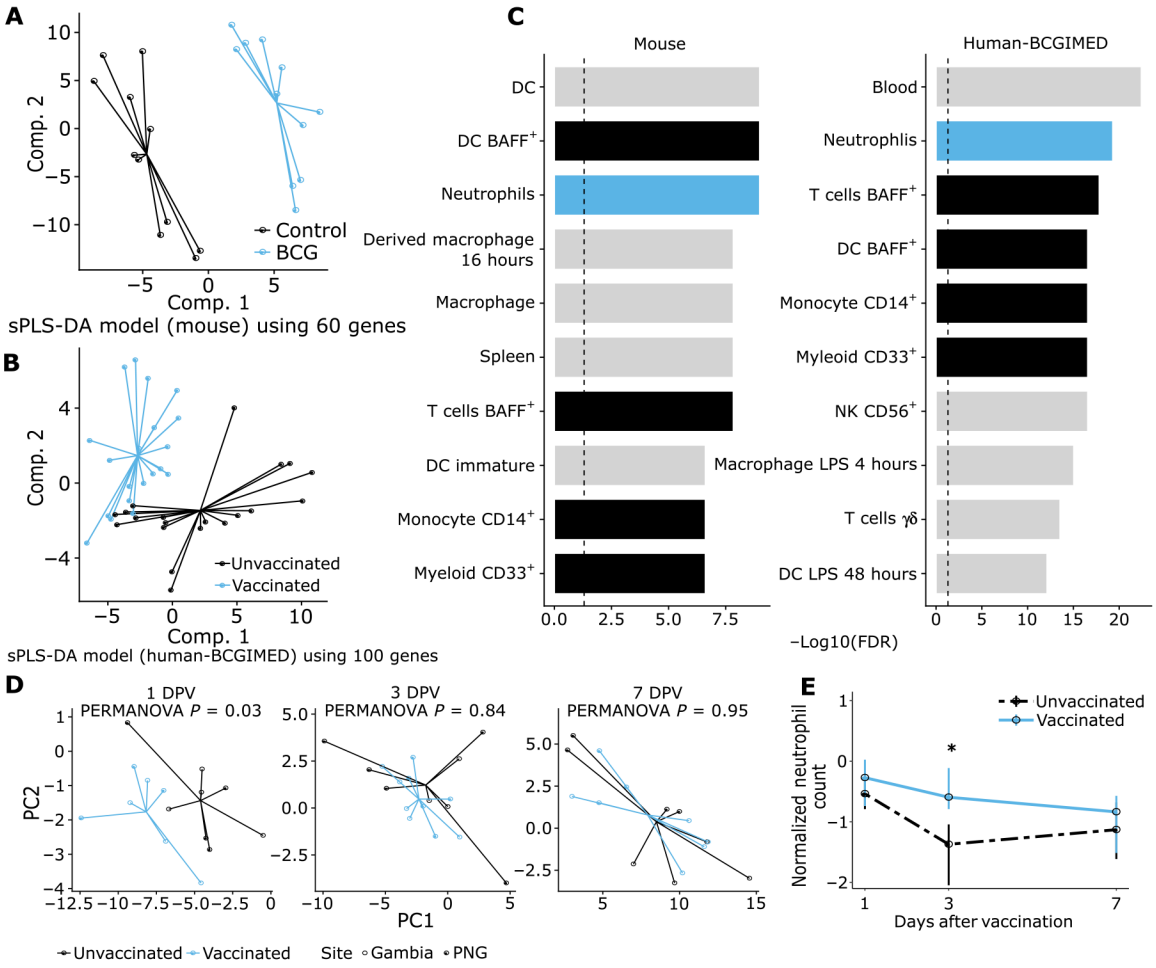


**Fig. 4. BCG vaccination induced EG in murine and human newborns.**

Transcriptional changes after BCG vaccination were identified by NanoString nCounter using sparse partial least squares discriminant analysis (sPLS-DA) in neonatal mouse (**A**) and human (**B**) peripheral blood 24 hours after vaccination ($n = 12$ mice, 60 transcripts; $n = 20$ humans, 100 transcripts; visualized using variate plots). (**C**) The top 10 pathways most affected by neonatal BCG at 24 hours after vaccination (determined through gene enrichment analysis) substantially overlapped between mouse (left) and human (right) (neutrophils marked in blue; other overlaps marked in black). DC, dendritic cell; NK, natural killer; FDR, false discovery rate. (**D**) Validation of BCG-induced EG signatures in two independent human newborn cohorts (The Gambia, West Africa; PNG, Australasia). The PCA depicts signatures for GM-CSF–induced changes in neutrophils, contrasting vaccinated (blue) versus control (black) separated by day after vaccination, with distinctness of the clusters tested using PERMANOVA. These gene signatures of GM-CSF–induced changes in neutrophils explained 89% of the variance observed between control and BCG-vaccinated newborns (calculated with 10 PCs). Similar patterns emerged for other EG-related gene sets shown in fig. S12. DPV, days postvaccination. (**E**) BCG increased human neutrophil numbers present on day 3 after vaccination in neonates from The Gambia and PNG (EPIC

cohort, $n = 6$ to 8 per group per time point, $*P = 0.02$, Wilcoxon rank-sum test, BH adjusted). Data are presented as medians with 25 to 75% IQR.